Stony Brook University

Mechanical Properties of 3-D Printed Cellular Foams with triangular cells

A Thesis Presented

by

Pratap Kumar Bunga

to

The Graduate School

in Partial Fulfillment of the

Requirements

for the Degree of

Master of Science

in

Material Science and Engineering

Stony Brook University

May 2014

Stony Brook University

The Graduate School

Pratap Kumar Bunga

We, the thesis committee for the above candidate for the

Master of Science degree, hereby recommend

acceptance of this thesis.

Dr. T A Venkatesh – Thesis Advisor
Associate Professor
Department of Materials Science and Engineering

Dr. Maen Alkhader – Thesis Co-Advisor
Assistant Professor
Department of Mechanical Engineering

Dr. Balaji Raghothamachar – Third Reader
Research Assistant Professor
Department of Materials science and Engineering

This thesis is accepted by the Graduate School

Charles Taber
Dean of the Graduate School

Abstract of the Thesis

Mechanical Properties of 3-D Printed Cellular Foams with triangular cells

by

Pratap Kumar Bunga

Master of Science

in

Department of Materials Science and Engineering

Stony Brook University

2013

In the present work, poly lactic acid (PLA) is used as a model system to investigate the mechanical behavior of 3-D printed foams with triangular cells. Solid PLA tension and compression specimens and foams made of PLA were fabricated using fused deposition 3-D printing technique. The solid PLA tension specimens were characterized for their densities and found to be about 10% lower in density as compared to their bulk counter parts. The triangular foams had a relative density of about 64%. The relationships between the structure of the foams and its deformation behavior under compression along two in-plane directions were characterized. Furthermore, simple finite element models were developed to understand the observed deformation behavior of triangular foams.

Table of Contents

List of Figures/Tables/Illustrations

List of Tables

Acknowledgments

I am deeply indebted to my research guides Dr. T.A. Venkatesh and Dr. Maen Alkhader for their support and guidance throughout the project. I would like to thank them for accepting me to be part of their research group and believing in me the entire duration. The time spent with the group has been an enriching and memorable experience.

A special note of thanks to Dr. Maen Alkhader for guiding and help me in carrying out experiments in Mechanical Engineering Department. The time bound approach and valuable suggestions of Dr. T.A. Venkatesh have also been pivotal in completion of the thesis.

I would like to express my gratitude to Doo Hee Lee, my fellow group member for helping me on various occasions during this process. His support during research days at Materials science department and Mechanical Engineering Department is greatly appreciated, without which it would have been very difficult to complete the project in time.

I would also like to thank Sumanthu in Mechanical engineering for helping me in the simulation work. Their tips and suggestions are very useful in obtaining better results.

Most importantly, I would like to thank all my friends and family members for their encouragement and support. Special thanks to my parents Satyanarayana Bunga and Tulasi Bunga for their unconditional love and support throughout the years.

Introduction:

Materials with low strength and stiffness that can be easily deformed under low stresses are typically referred to as Soft materials. Typical examples are polymers, polymer foams, metallic foams and granular materials. Soft materials have applications in the wide range and often we see in structural and packaging materials, shock-absorbers, vibration isolation devices, lightweight air-crafts, regenerator heat-exchangers and many more [1]. In addition to that a number of biological materials like bone, wood etc., are also called as Soft materials based on their mechanical response.

Dynamic behavior of materials is an area that studies the rapidly occurring changes in the material under rapid changing loads/forces (high-strain rates). The changes in characteristics of the material can significantly differ from the behavior under static or quasi-static conditions. Dynamic events require special study of inertia and inner kinetics of the materials becomes an important factor. In applications like aerospace, automobiles and transportation, packaging and other military services, understanding the material behavior under impact is as important as the static data. With this demand in the safety of structures and increasing demand of fast manufacturing techniques, it is necessary to improve the material properties at nominal and, as well as high strain rates. Scientific community has always sought to model the behavior of the different materials that were existing. Elastic, plastic and visco-elastic-plastic material models were developed and have been using in the description of the behavior of materials, and all those models need to test for which experimental apparatus have been extensively developed. Among this rigs, traditional tensile test is most used one to measure the quasi-static material properties while Split-Hopkinson Pressure bar (SHPB) became the most prominent tool in analyzing and in obtaining the dynamic behavior of materials in these days. This technique is used to obtain families of stress-strain curves for materials at high strain rates in between 102to104 s-1.

PLA material

Polylactic acid (PLA), also called as Polylactide is thermoplastic aliphatic polyester obtained from renewable resources, such as sugarcane, corn starch [2]. Two main monomers are used in the preparation of PLA: lactic acid, and the cyclic di-ester, lactide [2].

PLA has wide range of applications: it covers packaging materials, Nanotechnology, PLA food packing, in Nano composites and as Biomaterials [3]. It is a bio-resorbable polymer that is used in a number of clinical situations. It can be used as both bio-degradable and bio-compatible in contact with living tissues for examples biomedical applications such as implant, sutures, drug encapsulation, etc. It is also widely used as a feedstock material for 3D printers these days [4].

Tissue engineering applies many methods from materials engineering to create artificial constructs for regeneration of new tissue [5]. One common approach requires the use of a porous, bio-resorbable scaffold which serves as 3-dimensional template for initial stages of cell attachment and subsequent tissue formation afterwards under controlled conditions. The scaffold should have the following characteristics a) porous with interconnected network b) bio-compatible and bio-resorbable c) suitable surface chemistry for cell attachment and d) mechanical properties that could match those of tissues [6]. Fig.1 shows some Scaffold structure prepared in Orthopedics Lab of Standford University using 3D printing technology. PLA is one such material being considered that satisfies many of tissue engineering requirements and offers ease in the manufacturing process. Also, nano materials in combination with PLA structures can create new PLA nanocomposites with greater abilities.

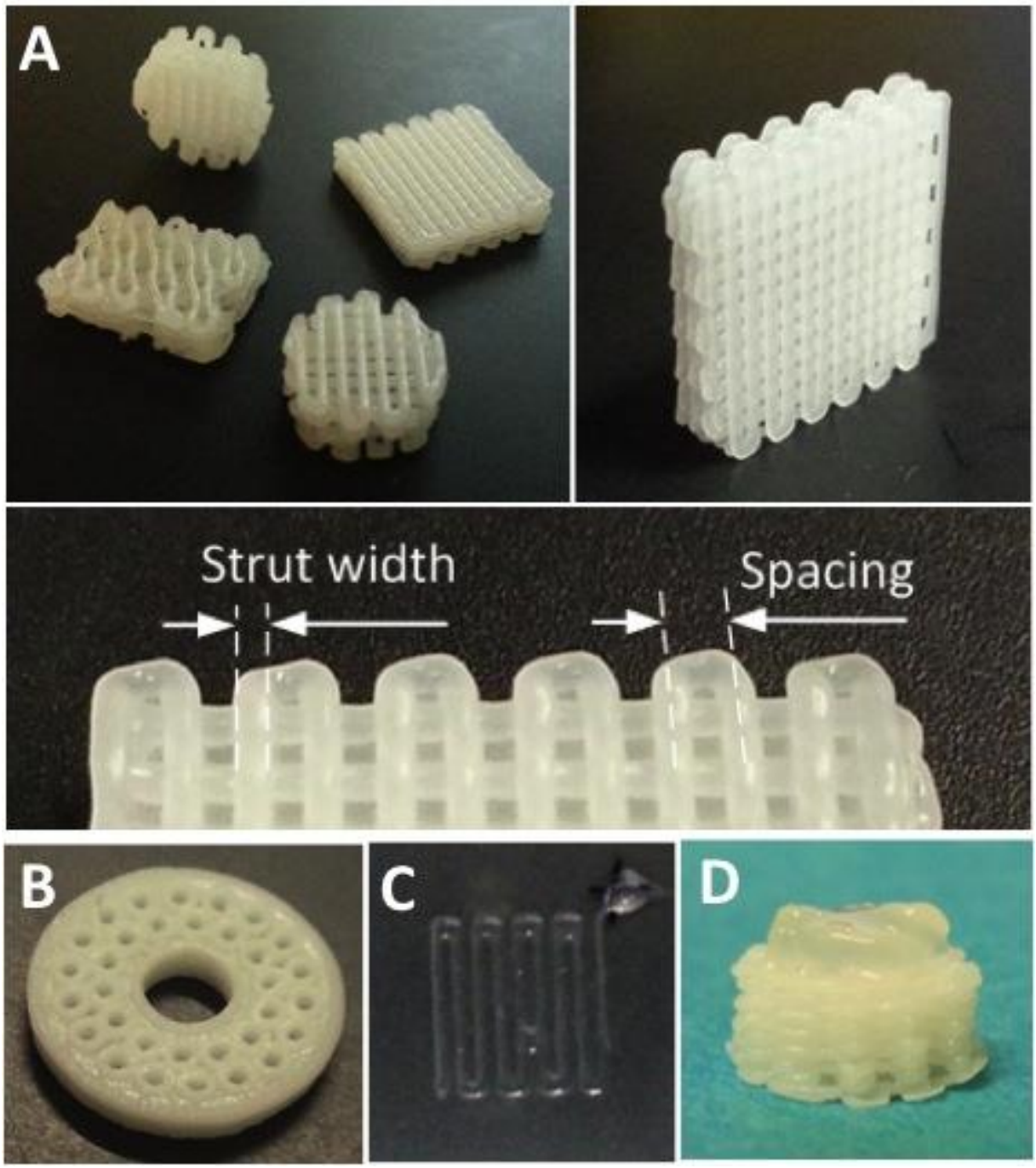

Fig.1. Scaffolds made using 3D fabrication system. A) Porous ceramic composite B) bone like scaffold C) latticed hydrogel scaffold. D) Hybrid hydrogel composite

Many processing techniques have been developed to fabricate 3D scaffolds that include solvent casting, melt molding, temperature induced phase separation. However, no computer allowed

process has allowed researchers to fabricate scaffolds of high quality [6]. The imperfections of these techniques have encouraged scientists to look into applying proto-typing technology of 3D printing by Fused-deposition Modelling [2]. It builds complex structures layer by layer allowing almost unlimited designs and a wide variety of materials that can be used Scaffold engineering.

For a printed PLA structure to use as a scaffold, mechanical properties of the printed materials and structures need to be evaluated. The need to understand the physical and mechanical properties in between the original PLA material and printed PLA is needed to understand. PLA and polymer blends were tested under quasi-static and dynamic conditions using SHPB. A trend of mechanical properties difference by varying the composition of polymer blends was discussed [7]. However, the samples were prepared by conventional hot pressing technique in industry. Experiments on printed 3D PLA for the mechanical properties by was done by Giordano, Russell A [8] under quasi-static conditions.

In this study, a series of experiment and simulations techniques were conducted to test the printed PLA material in both static and dynamic conditions. Models of porous cellular 3D structured PLA (Triangular cell) are created and printed through 3D printer for mechanical property evaluation.

1. Cellular Materials

A cellular solid is an interconnected network made up of plates or struts that form the faces and edges of cells. There are several man-made and natural occurring cellular structures. Bones, wood

are natural occurring cellular materials and may also refer to as soft materials. Cellular materials have interesting combinations of physical and mechanical properties; lot of attention has been given to soft and cellular materials owing to their good shock mitigation, energy absorption and vibration isolation which have wide applications in automotive, aerospace and transportation and biomedical applications [10]. Cellular solids especially are used as energy absorbers especially with high impact in blast and crash protection. This is because during the plastic compression at the plateau stress, they have large densification strain [11]. Their low specific weight in conjunction with high stiffness is valuable combination for many applications.

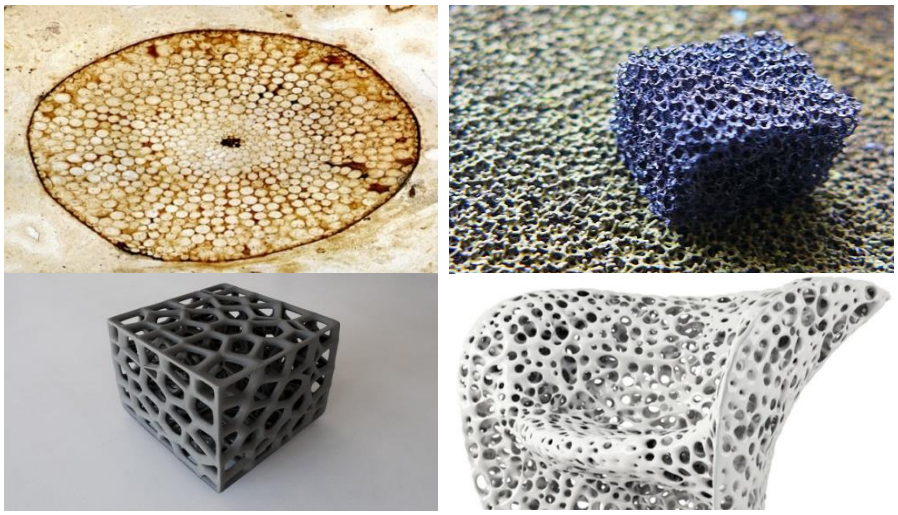

Fig.2. Showing cellular architectures of a) wood b) regenerator in heat-exchangers c) artificial foam d) bone marrow

Among those cellular, a periodically cell-structured materials were well noticed in the R&D. Due to their regular micro-struss architecture and 2D periodic channel, they show superior mechanical properties than foams. These are rationally adaptable to the engineering applications since the mechanical behavior is predictable by using unit cell modelling and homogenization theory. Shape

of the cells has an important role; the mechanical response is determined by the individual cell structure and configuration and the matrix properties. Different periodic cellular arrangements have been studied to optimize the core structures (Fig. 3). Of these, Honeycombs have been widely studied for many applications. In particular, Gibson et al. [3] studied the mechanical behavior of hexagonal honeycombs. He mentioned the effect of cell wall thickness and relative density on the stress–strain response and also represented elastic anisotropy as a function of in-plane directivity for square, triangle and hexagonal unit cell structures [2, 3].

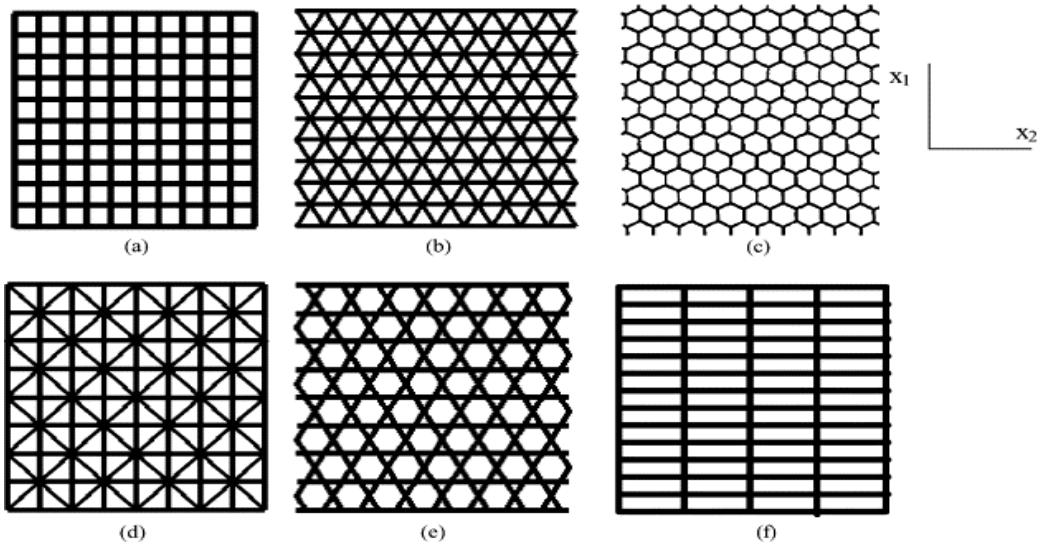

Fig.3. Honeycombs with different cell shapes, including: (a) square, (b) triangles arranged as hexagonal super-cells, (c) simple hexagonal, (d) mixed triangular and square (e) kagome, and (f) rectangular.

1.1 Prior Work on Honeycombs

1.1.1 Static & Dynamic Crushing

In quasi-static crushing of cellular materials, every individual cells can exhibit a wide range of behavior resulting from the elastic deformation, buckling and plastic collapse of the cell walls. The deformations in different cells interact with each other resulting in complex patterns of deformation. Localization is a characteristic feature of the compression behavior of cellular materials. Collapse takes place at the weakest row or band of cells first and gradually spreads to stronger areas of the structure. This process generates a nominal stress–strain curve which, overall, is convex towards the strain axis in the post-yield (plateau) and densification regimes.

Crushing of a cellular material under impact (suddenly imposed boundary velocity) conditions is quite different from its quasi-static counterpart; the crushing behavior is dominated by structural and dynamic/inertial effects for moderate impact velocities and by stress wave propagation under relatively high impact velocities. Enhanced compression strength of the wood under dynamic conditions is reported by Reid and Peng [13]. Aluminum foams also showed a similar trend under dynamic conditions was reported by Tan [14]. Honig and Stronge reported a strong increase in total dissipated energy with increasing impact velocity through finite element analysis [15]. Localization is even more in the dynamic crushing than those in the quasi-static crushing. When the impact velocity is high, crushing wave front forms at the impact end and travel through the cellular structure. While the cells behind the crushing front are fully crushed, the cells in front of it remain undeformed. The deformation pattern is reminiscent of a propagating shock.

The stress–strain curve of uniaxial compression of cellular material possesses the feature shown as a fine line sketched in the Fig. 4. The pattern of the deformation is identified by three stages, a short elastic stage, a long plateau stage and finally a densification stage. Reid and Peng [13] are

the first to propose a rigid–perfectly-plastic–locking (R–P-P–L) model for the cellular material shown in Fig 4. They had derived the equation for the dynamically- enhanced stress of the cellular material under dynamic loading which is based on shock wave theory. This theory says that crushing stress is direct proportional to the square of the impact velocity (below equation) and this theory models were well verified with experimental data (Crushing of wood grain by Reid and Peng) [13].

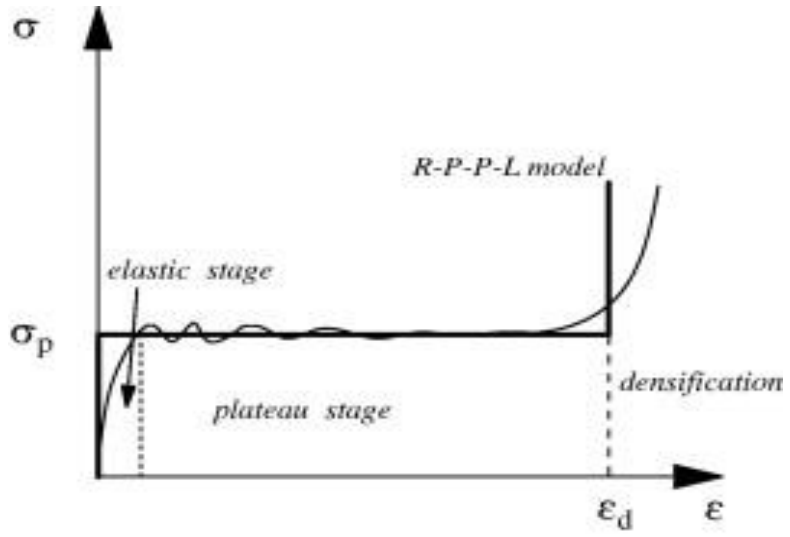

Fig.4. Stress-strain relationship for the cellular material

$$\sigma_d = \sigma_p + \frac{\rho_0}{\varepsilon_d} V^2$$

where $\boldsymbol{\rho_0}$ is the density, $\boldsymbol{\varepsilon_d}$ is the locking strain (densification), *V*- Impact velocity and $\boldsymbol{\sigma_p}$ is the quasi-static plateau stress of the cellular material.

Parameters such as porosity, cell shape and its stability, side length and thickness are very important; In fact, other minor topological aspects of cell shapes, such as the edge connectivity,

number of contact neighbors will vary from one structure to another, and influence the properties in significant ways specially when the impact loading is applied, the high frequency components will control the dynamic response of the structures. The influence of the cell topology on the local stress dynamic evolution becomes more dominant [14]. As such, clarification of the relation between the cell local arrangement and material dynamic behavior is also an important task in the dynamic description of honeycombs.

1.2 Triangular Structure

These are periodic honeycombs with equilateral triangular cells inside structures. Triangular honeycombs are stiff under both bulk and shear compression; indeed many civil engineering constructions like bridges are often based on triangular geometry. An important piece of work was done by Ying, Xin-Chun [16], did test on triangular structures by varying speeds from 10 to 70 m/s. The response of the triangular structure also follows basic rules of any other cellular structures. At the initial stage the response is linear and with further crushing, the deformation mode becomes plastic. When the stresses go beyond the plastic limit of the matrix material and the plastic hinges form at the cell walls at which the stress reach the peak of the elastic limit. The crush front of the triangle propagates different than the other cells like honeycomb that have diagonal shear bands or 'X' mode formation [17]. Localization starts from the edges of the cell and slowly propagates to the center. Fig.5 shows the response of triangular cells in-plane compression in a velocity range of 10 to 70 m/s.

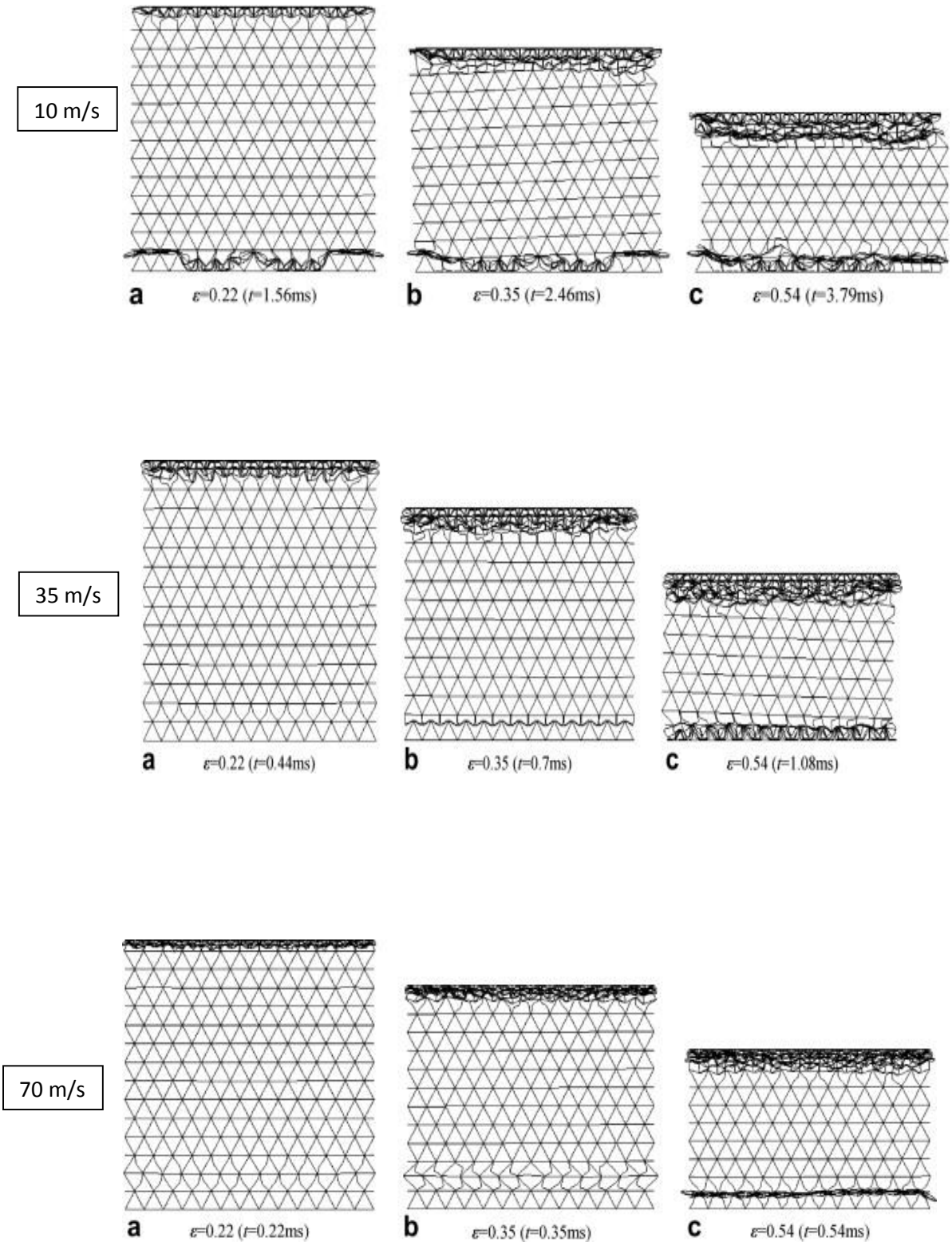

Fig.5. Deformation modes of triangular honeycombs at velocities of 10, 35 and 70 m/s

Kanyatip Tantikom and Tatsuhiko Aizawa [18] gave clear demonstration of how the deformation starts from the individual cell based on their computational and theoretical models. The cell walls in the triangular cell-topology bend around their vertices in their elasto-plastic response during crushing as shown in the Fig 5. A shear band forms as this bending deformation propagates to adjacent triangular connectivity. The deformation mode changes from uniform compression to asymmetric deformation with bent-shear collapsing. Different number of localized deformation bands causes anisotropic plasticity. Formation of a single bent-shear-mode localized deformation band lowers the yielding and plateau stresses. On the other hand, the yield stress increases due to the work-hardening in the post-localization regime (formation of several localized deformation bands). This needed additional plastic work to be done for the propagation of this bent-shear-mode localization.

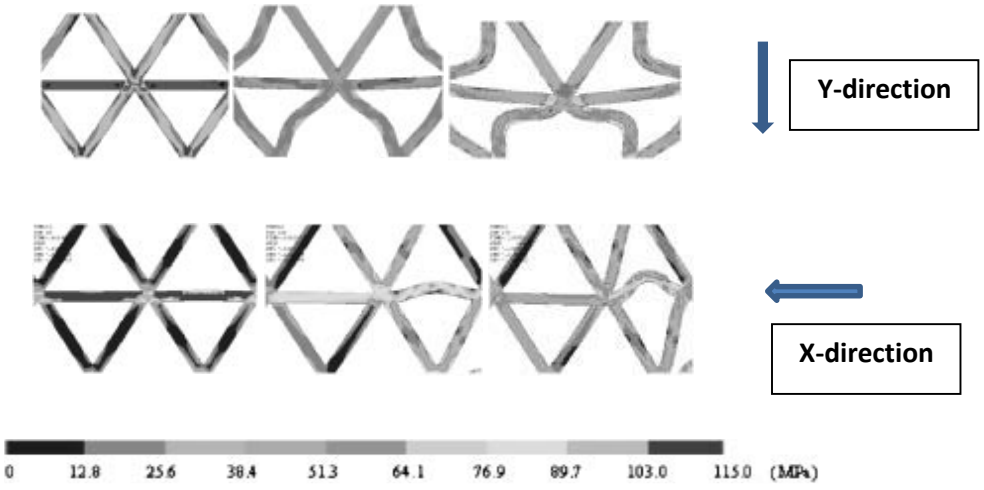

Fig.6. Stress-contours and shear localization develop in the triangular cell structured Honeycomb

Figure 9 shows stress contour in the cell walls of deformed cells. In the case of loading in Y direction, diagonal legs converging towards center in the lower half only bent in the post-yielding to form a pair of localized deformation bands in 45 degrees. No significant bending occurs in other four columns (remaining four edges in the block). This leads to the formation of bent-shear mode localized deformation. On the other hand in X-direction, the stress contours begin at the corners of the triangle as shown in Fig 6. In this mode, only one edge is collapsing and others never collapsed (the base side of the two triangles). After, this edge collapses; it forms the bent-shear-mode localized transformation and transfers the deformation band to the next row.

2. SHBP

The split Hopkinson pressure bar technique is extensively used to characterize material behavior at high strain rates. The split Hopkinson pressure bar (SHPB) (Kolsky 1949), or Kolsky's apparatus [19] has become today a very popular experimental technique for the study of the constitutive laws of the materials at high strain rates.

While the traditional tensile test is the major test to measure the quasi-static data, Split Hopkinson Pressure Bar is the chief experimental technique to obtain dynamic properties of the material with which the characteristic of compression deformation, energy absorption and strain rate sensitivity of metal foams have been intensively investigated [19].

An application of the split Hopkinson pressure bar to the dynamic testing of materials is given whereby continuous records of the strain vs. time, strain rate vs. time, stress vs. time, and stress vs. strain may be simultaneously recorded. The materials studied with SHPB in the past decades are often metals, the plastic behavior and rate dependence of which have been of the main interest. However, as SHPB has enjoyed an increasing popularity in metallic materials, it is also applied to many non-metallic materials such as concrete, rocks, salt-rock, polymers and polymeric foams. Characterization of strain rate effects on the mechanical properties of materials requires experiments over a wide strain-rate range. In practice, quasi-static testing frames can achieve strain rates up to 100 s^{-1} with close-loop controls on the testing conditions; whereas dynamic experiments with a split Hopkinson pressure bar (SHPB) are conducted at strain rates from 10^2 to 10^4 s^{-1}.

2.1 Theory and Design of SHPB Experiment

A conventional SHPB apparatus consists of a gas gun, a striker an incident bar, a transmission bar, an energy absorption device and a data acquisition system. Specimen is sandwiched in between the incident bar and transmission bar. A gas gun that contains compressed gas launches striker on to the incident bar that generates elastic waves in both incident bar and striker. The elastic wave in the incident bar is called *incident wave*. The incident stress wave generated travels down the bar and is recorded by the strain gauges mounted longitudinally on the bar. Due to the mechanical impedance mismatch between the bar material and the specimen, the stress wave then passes through the specimen and the specimen is compressed. Part of the stress wave is reflected in the form of a tensile pulse and is called *reflected wave*. Part of the wave energy is absorbed by the specimen and the remainder is transmitted to the transmitter bar and recorded by the other strain gauge mounted on the transmitter bar as a *transmitted wave*. The three readings are used to determine the time dependent stress state of the specimen [20]. The incident and reflected wave signals are sensed by the strain gage on incident bar whereas the transmitted signals are sensed by the strain gages on the transmission bar. All the three signals are recorded with a digital oscilloscope. From the time dependent strain state data obtained from the signals, a stress vs. strain plot can be plotted.

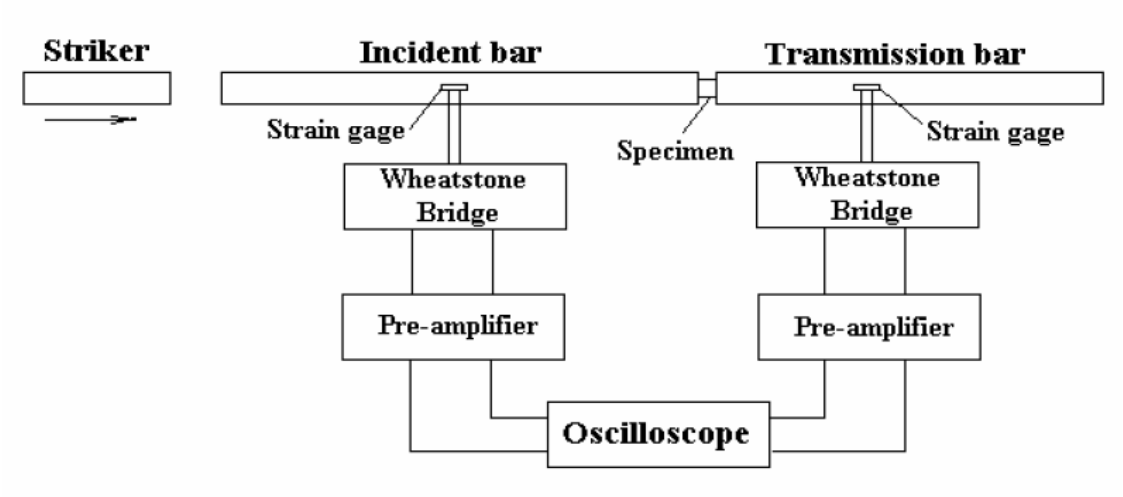

Fig.7. A schematic of Conventional SHPB setup

Dynamic Stress Equilibrium Process

Dynamic Equilibrium Stress is achieved when the waves in the specimen traverse several times, causing the specimen to ring up to near a uniform stress such the specimen deform under constant flow stress. In order to perform SHPB experiments, achieving to constant flow stress is a must. Equilibrated Stress is so important in this experiment because the non-equilibrated stress may lead to a drastic non-uniform deformation in specimen which can invalidates the experimental results for the material property characterization. Dynamic Equilibrium Stress can be achieved quickly in metallic or ceramic specimen due to the high wave speeds in those specimens relative to the soft materials.

Mathematical Model:

SHPB analysis is based on some basic assumptions. (i) The waves propagating in the bars can be described by the one-dimensional wave propagation theory. (ii) The stress and strain fields in the

specimen are uniform in its axial direction. (iii) The specimen inertia effect and the friction effect in the compression test are negligible.

One dimensional stress-wave analysis on the bars determines the strain, strain rate and stress histories in the specimen,

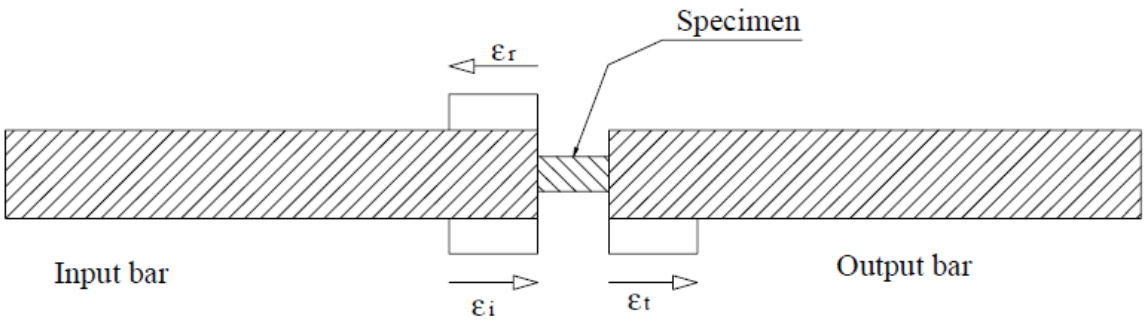

Fig.8. Working Principle of the SHPB

$$\dot{\varepsilon} = \frac{C}{L_s}[\varepsilon_i(t) - \varepsilon_r(t) - \varepsilon_t(t)] \quad \text{---------- (2)}$$

$$\varepsilon = \frac{C}{L_s}\int_0^t [\varepsilon_i(t) - \varepsilon_r(t) - \varepsilon_t(t)]dt \quad \text{---------- (3)}$$

$$\sigma = \frac{A_0}{2A_s}E_0[\varepsilon_i(t) + \varepsilon_r(t) + \varepsilon_t(t)] \quad \text{---------- (4)}$$

Where $\varepsilon_i(t)$, $\varepsilon_r(t)$ and $\varepsilon_t(t)$ are incident, reflected and transmitted strain histories measured by the strain gages.

E_0 - Young's Modulus of the bars C - Elastic bar wave speed, A_0 is the cross section area of the bars
A_s and L_s are initial cross-sectional area and length of the specimen respectively.

After simplifying the above equations the nominal strain rate and nominal stress in the specimen are given by,

$$\dot{\varepsilon} = -2\frac{C}{L_s}[\varepsilon_r(t)] \quad \text{---------- (5)}$$

$$\boldsymbol{\sigma = \frac{A_0}{A_s} E_0 \varepsilon_t(t)} \quad \text{---------- (6)}$$

Equations 2, 3, 4 are based on the assumption of dynamic stress equilibration in the specimen. From these 5, 6 equations we can plot the stress-strain profile of the specimens.

Instrumentation:

Typical instrumentation of SHPB setup includes strain gauges, an oscilloscope or a transient recorder, an electronic integrator or an operational amplifier, a trigger circuit, power supply and a velocity measurement system. The Oscilloscope or transient recorder is used to record the strain signals from the strain gauge stations. The reflected signal can be integrated with the amplifier and the result is the signal proportional to the specimen strain. This can be input to the X-axis of the recording instrument and the transmitted signal is input in the Y-axis. The recorded profile will allow direct visualization of the profile of the stress-strain curves of the material.

To determine the Striker impact velocity, a velocity measurement system is used. The most common measurements employed are a time interval counter associated to either a magnetic pick-up or photocells and light sources.

Fig.9. Experimental set-up of SHPB in our lab

Data Analysis and Micro Structure:

A high speed digital camera is generally used to observe the deformation process of the material or structure. It helps to find the deformation pattern of the specimens.

Dynamic Stress-strain curves are obtained after the mechanical loading, and of the most cases are desired to be collecting the specimens for microstructural investigations. Loading histories need to be correlated to the microstructure evolutions in order to build up accurate correlation between the macroscopic mechanical properties and the microstructures of the sample.

2.2 Modification of SHPB

When soft, cellular materials have gained importance in the construction, design and automobile industries, these materials increasingly investigated are subjected to impact testing. Although SHPB has several advantages for dynamic characterization of materials, testing soft materials poses some challenges. There are many uncertainties that may invalidate the resultant stress-strain data for soft materials on a conventional SHPB test. To conduct valid SHPB experiments, Uniform stress distribution in the specimen is a fundamental requirement. Soft materials are often characterized with low modulus and mechanical impedance and hence have low wave speeds. It is very difficult to achieve dynamic equilibrium within the timescale of a dynamic test especially for soft materials [20].

In order to get a valid data for Soft materials, these are three requirements:

1) Accurate transmitted signal
2) Dynamic Stress Equilibrium
3) Constant Strain rate deformation

Over years, several modifications have been made to SHPB experiments to accommodate soft materials and cellular materials that include the use of low impedance polymeric bars [21], quartz force gages [22], pulse shaping [23] and changes to specimen geometry, including reduced thickness [23, 24].

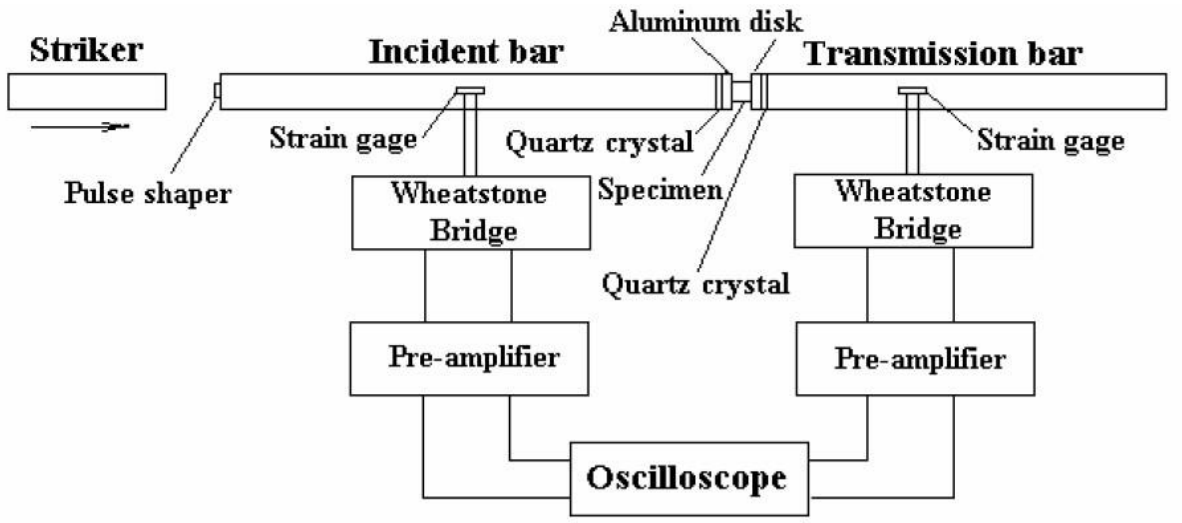

Fig.10. Modified Split-Hopkinson pressure bar test that has pulse-shaper, Aluminum disks

Sensing weak transmitted Signal

Due to the low modulus and mechanical impedance of soft materials, it would result in poor data from transmitted signals. Based on the study, it is recommended to have less mechanical impedance difference between the bar and the specimen materials. Guideline of selecting bar material for soft-material testing is provided by Gray and Blumenthal [25].

Since Polymeric bars have lower mechanical impedance, they gained importance in testing soft materials. They can sense the weak transmitted signal with high resolution. PC, PMMA are most common materials used for test foam materials and rubber. However, these materials don't exhibit linear elastic behavior. The resultant data brings uncertainty as it causes significant stress wave dispersion and attenuation due to the viscoelastic properties [26]. An accurate model is necessary to develop and Sawas et al. [27] presented a detailed model of correcting the visco-elastic waves and calculating the stress-strain data.

Such kind of uncertainities by the visco-elastic bars can be avoided by using aluminum bars [28], magnesium bars, and titanium bars. Aluminum bars are the most common among the low impedance metallic materials**.** Employing quartz-crystal transducer is the also one of the most efficient way to get high signal to noise ratio waves. Another efficient method is to employ high sensitive strain gauges like semiconductor strain gauges. The semiconductor gauges detects weak transmitted signals with high accuracy [29].

Achieving Dynamic Stress Equilibrium and Constant Strain Rate

Wave speed in the material plays an important role in reaching the dynamic stress equilibrium; the process is faster in the specimen that has higher wave speed than in a one with low speed. Soft materials are the ones with low wave speed which increases the time to reach to Dynamic equilibrium.

Specimen thickness: has effect in controlling the Dynamic equilibrium as pointed out by Kolsky in his early experiments. Song and Chen also have also extensively investigated on the specimen thickness which they performed in EPDM rubber specimens and RTV 630 which demonstrated that decrease in the specimen size has an effect on Dynamic Stress equilibrium [23].

Pulse Shaper: Pulse shaping technique was introduced to reduce the attenuation of the waveforms to smooth pulses that improve the resolution of the stress-strain curves. Design of pulse shaper is shown in Fig. 10. A dummy specimen is placed the end of the incident bar in which the striker impact facilitates constant deformation rate in the specimen. Alternative pulse shaping technique is to a place tip material in between the striker and the incident bar. Copper is most common material used in pulse shaping technique [30].

3. Experimental

3.1 Material and 3D printer

Recently, a 3D printer called *Replicator 2* was developed and commercialized by MakerBot, which uses natural polymers to build the structures. This commercial machine was used for the study; this printer uses Fused Filament Deposition (FFD) technology originally was developed at the Massachusetts Institute of Technology (MIT) [31]. The FFD is a layered fabrication process, in which the sliced 2D profile of a computer model is printed using the plastic filament unwound from a coil. Successive 2D profiles are then printed on a freshly laid layer until the whole model is completed (Shown in Fig 11)

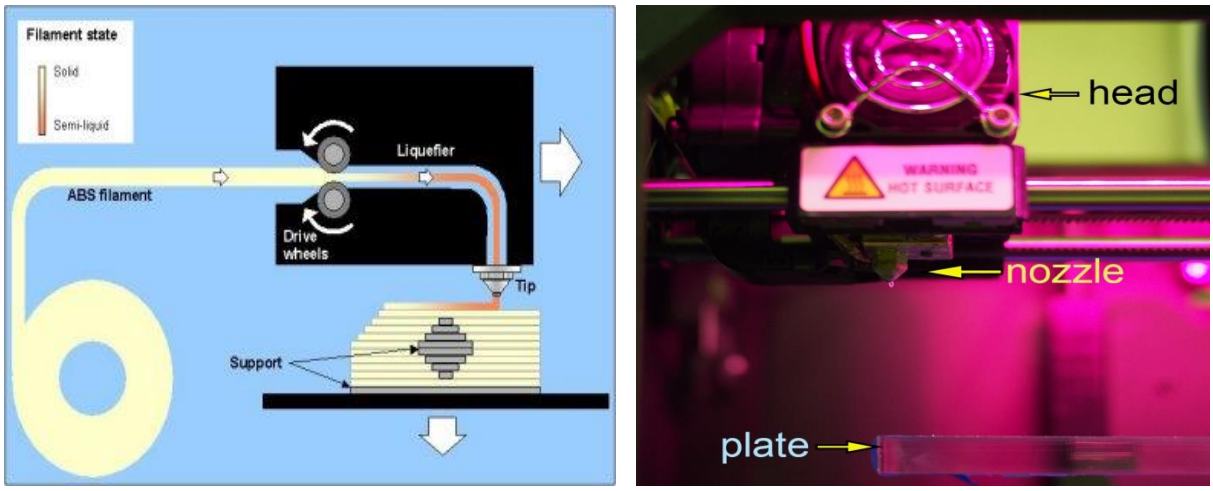

Fig.11. Fused deposition modelling: – nozzle ejecting molten plastic on to the plate

The model is produced by extruding drips of thermoplastic material to form layers. A plastic filament is unwound from a coil and supplies to an extrusion nozzle that pushes filament to print

layers at a controlled rate. The thermoplastics are heated past their glass transition temperature and are then deposited by an extrusion head. The nozzle is initially heated to melt the material and hardens immediately after extrusion from the nozzle.

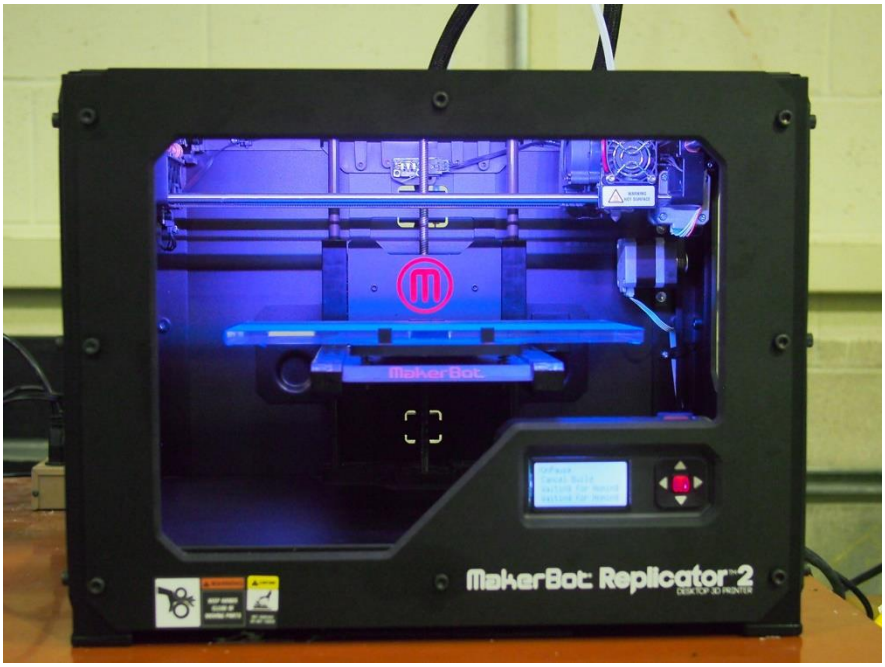

Fig.12. MakerBot's *Replicator 2* printer from our lab.

The nozzle moves both horizontal and vertical directions controlled by a numerically mechanism where tool-path set by a computer-aided manufacturing (CAM) software package called MakerWare originally by the MakerBot company itself. We used PLA material in design and building the structures for the experiments. Properties of PLA are listed in table.

Chemical name and CAS Number	Polylactide resin (9051-89-2)
Glass Temp	60~65° C (140~149° F)
Melting Temp	150~160° C (302~320° F)
Density	1.24 g/cc
Yield Strength	50-55 MPa
Young's modulus	3- 3.5 GPa

Table 1: Properties of PLA material

3.2 Design and Fabrication

In this study, models are designed using CAD software (Solid Works v. 12.0). Four different designs are prepared. A cylinder, dog-bone specimen, honeycomb and triangular structures made using 3D printer, shown in the Fig 13.

The designs were exported in a prototyping format (.stl file format) for the 3D printer to read. The ’stl’ files were uploaded to the 3D printing Maker ware software where the model was sliced by a slicing algorithm. These 2D sliced layers were then built layer by layer until the final object was physically formed completely.

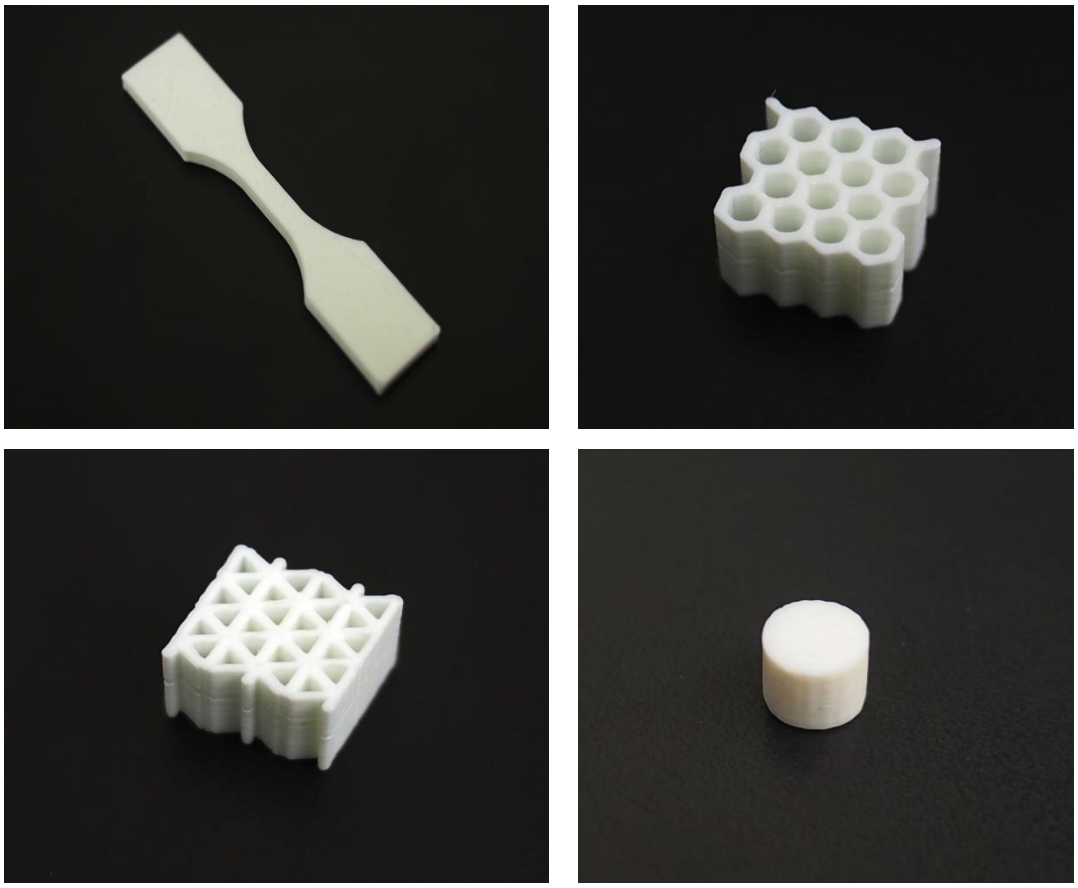

Fig.13. a) Dog-bone b) Honeycomb c) triangular and d) Cylinder prepared from 3D printer

The designs parameters we used to build the structures are included in the following table:

Layer height	between 0.1 to 0.2mm
Infill	100 %
Temperature	230 ºC
Speed while extruding	90 mm/sec

Table 2: Parameters used in 3D printing

3.3 Tension Test

The quasi-static axial tension experiments are performed according to the ASTM standard test method for tensile strength and Young's modulus of the printed PLA material. Dog bone specimens were used in this experiment to measure the properties. A dimensioned drawing of the tension specimen can be found in figure 14. The specimens gauge length of 10mm is used as the working area and the stress is calculated with area of cross-section of the gauge length. Low rate tension experiments were completed using the *Tinius Olsen 1000* machine of 1000 pounds per inch force of loading capacity.

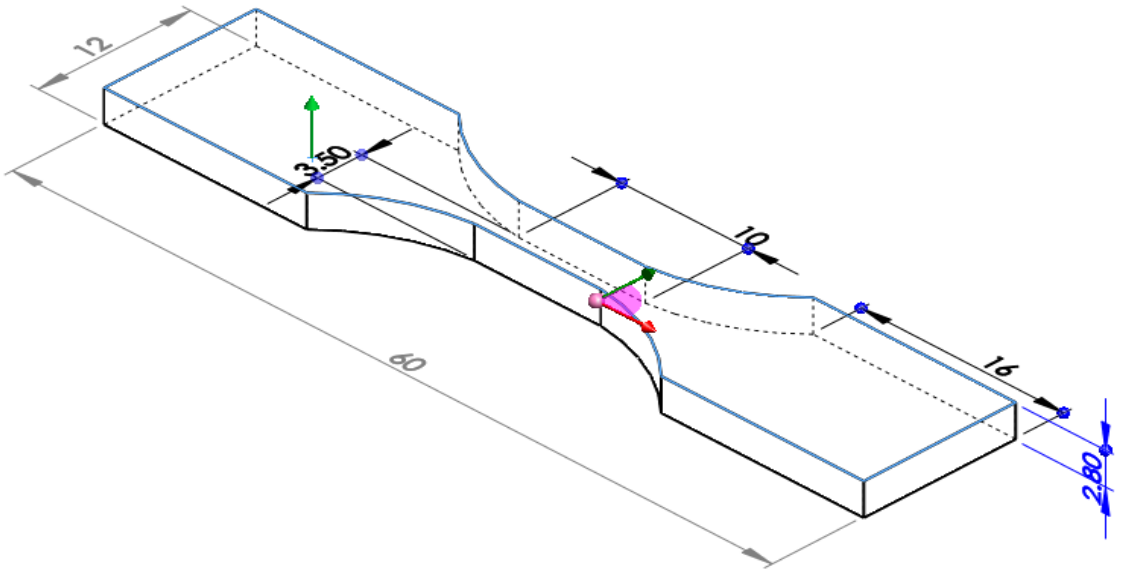

Fig.14. Dimensioned drawing of Tensile Dog-bone Specimen (Units: mm).

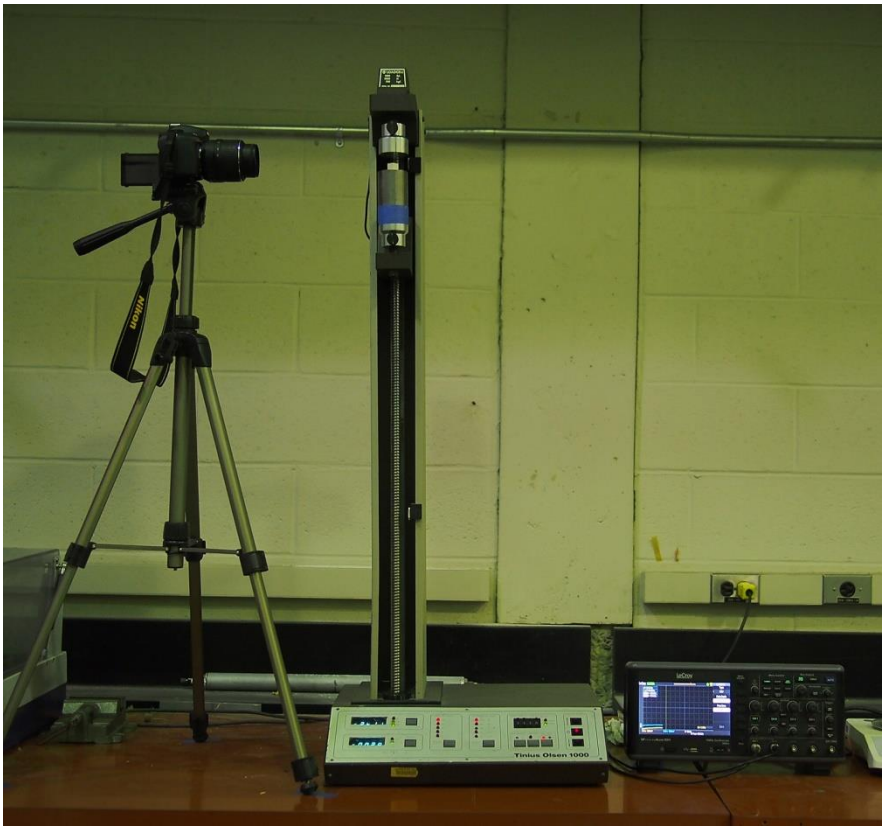

Fig.15. Experimental set-up for tensile and compression test

The specimen edges are accommodated into the threaded collars of actuator arms of the load frame. A Nikon D5100 digital camera was used to record the change in the length of the samples during test and to provide a confirmation of measured strain. A total of 4 specimens were manufactured and tested as the part of this study at different loading rates. We did experiments at speed rates of 0.01, 0.05 and 0.1 inch/min. Stress-strain plots were plotted based on the Force-displacement signals obtained from the oscilloscope.

3.4 Compression Test

A series of compression tests were performed on the Cylindrical and Triangular honeycomb specimens.

Cylinders: A total of 6 specimens were fabricated using 3D printer, dimensioned drawing of the cylindrical specimen can be found in the Fig 16. Quasi-static compression test was performed using the same machine and the experimental set-up mentioned above in tension test to evaluate the Yield strength and modulus.

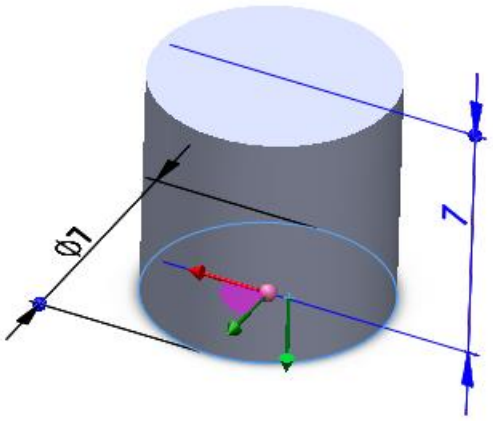

Fig.16. Dimensioned drawing of a cylinder (Units: mm).

The experiments are performed with displacement control mode and properties are evaluated for loading rates of 0.01, 0.05 and 0.1 inches/min, deformed configurations are recorded using a Digital camera. The loading rate is carefully chosen in a way that it is closest to quasi-static loading conditions (below 0.1 inches/min) and does not result dynamic effects on the specimen.

Triangular Cell Structure:

The structure is composed of 8 cells in the X direction and 4 in the Y direction. The thickness of the walls is 0.6mm according to the CAD model we made. Quasi-static Compression tests were carried out by the Universal Testing machine mentioned in the above at the room temperature. In-plane compression tests were performed for the matrix stiffness, and to deformation pattern.

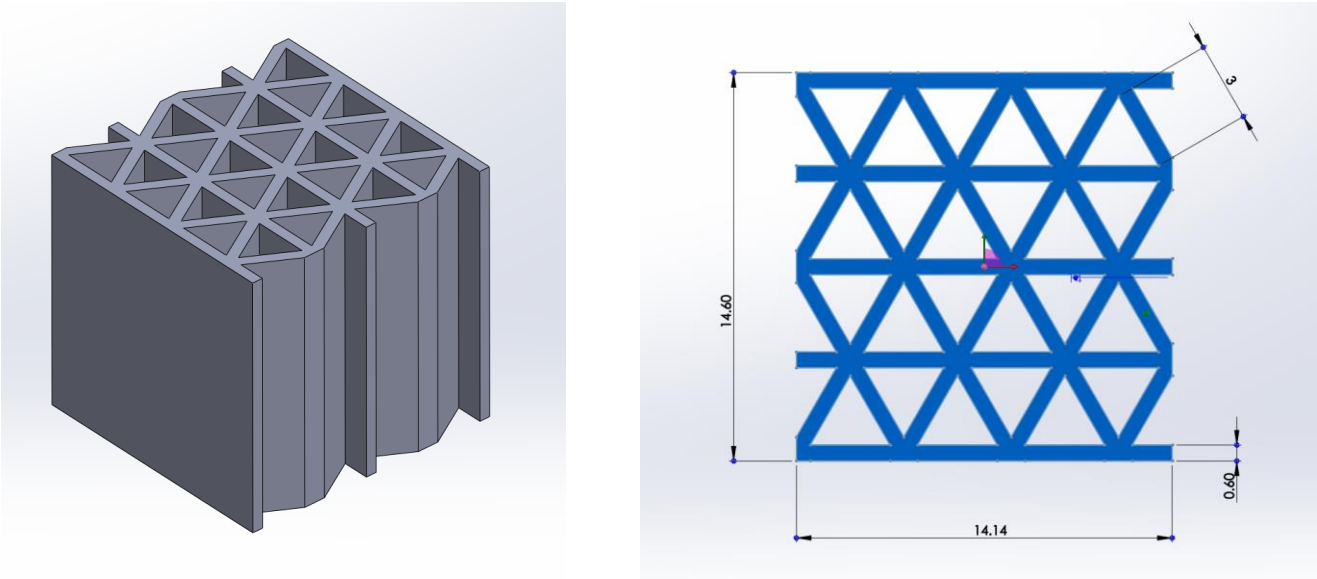

Fig.17. Model and dimensioned drawing of triangular honeycomb (Units: mm).

A total of four specimens were prepared to test at quasi-static rates of 0.05 and 0.1 inch/min in both X direction and Y directions shown in Fig 18. The deformed configurations were taken by digital camera during testing. Stress-strain plots were drawn using the Force-displacement data given by the instrument.

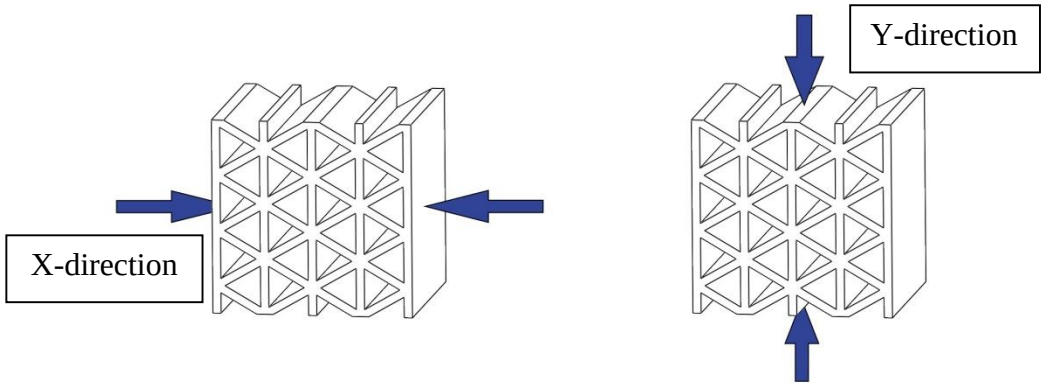

Fig.18. Model showing the direction of Compression.

3.4 Simulation

An in-plane crushing of 2D triangular-cell honeycomb are modelled using finite elements to explore the static and dynamic response of the cellular materials and to investigate the features of the crush front and deformation pattern. A commercially available software package, ABAQUS v.12 was used for simulation. The model had about 22847 nodes comprising of 22800 elements. The parent material is assumed to be elastic, perfectly plastic with E = 1.67 GPa and v = 0.36, where E and v are Young's modulus and Poisson ratio of the material respectively. The above values are derived from the compression test of the cylinders.

The density of the parent material and thickness of the wall are 1.24 g/cc and 0.6mm. The cell is regular with the same value of edge length, which is 3 mm, and the corresponding angle between the edges is 60º.

4. Results and Discussion

4.1 Evaluating the properties of the printed PLA Material

Tension and compression tests were performed on solid PLA specimens that were fabricated using 3D printer to find out the mechanical properties of printed PLA (Young's modulus and yield strength).

4.1.1 Tension

When Uni-axial tension test is performed on specimens, the nature of deformation of some samples is dissimilar with other specimens. Most of the samples showed a brittle behavior, fractured around 4 % strain which can be comparable with the original PLA material. However, some samples showed an elongation of more than 10 % which so uncommon (Fig. 18(b)).

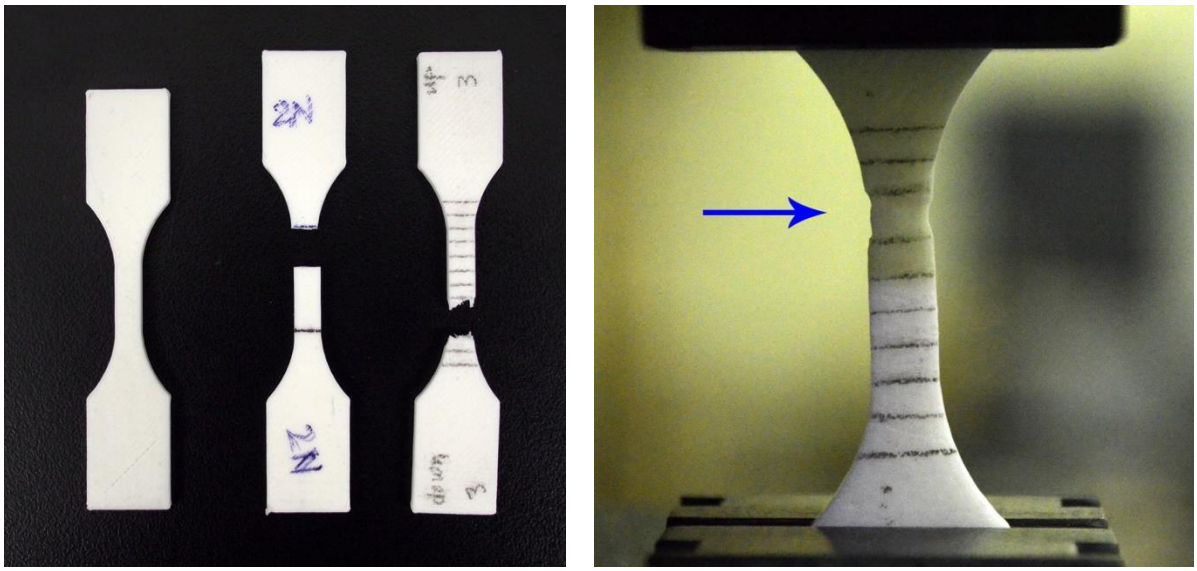

Fig.19. a) shows the specimens after tensile test **b)** necking during the tensile test

The figure shows the Stress-strain profile of tensile sample at a loading rate of 0.05 inch/min, the yield strength is in between 40-50 MPa and the Young's modulus is 2 Gpa.

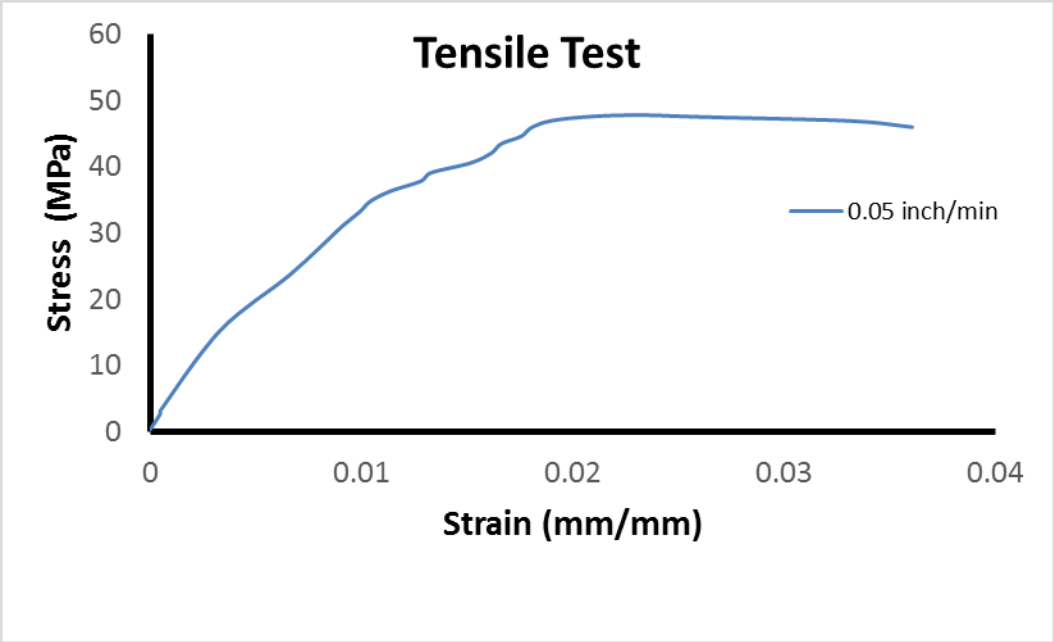

Fig.20. Stress-strain curve of a tensile specimen at a loading rate of 0.05 inch/min

4.1.2 Compression

Compression tests were originally done at 0.01, 0.05 and 0.1 inch/min loading rates. The stress-strain profiles of these specimens showed almost a similar profile irrespective of their loading rate. Fig. 20 shows the stress-strain profiles of the cylinder samples tested. The yield strength varied from 52 - 67 MPa whereas the Yield strength is 1.45- 1.8 GPa is observed through the compression experiments of the cylinder specimens.

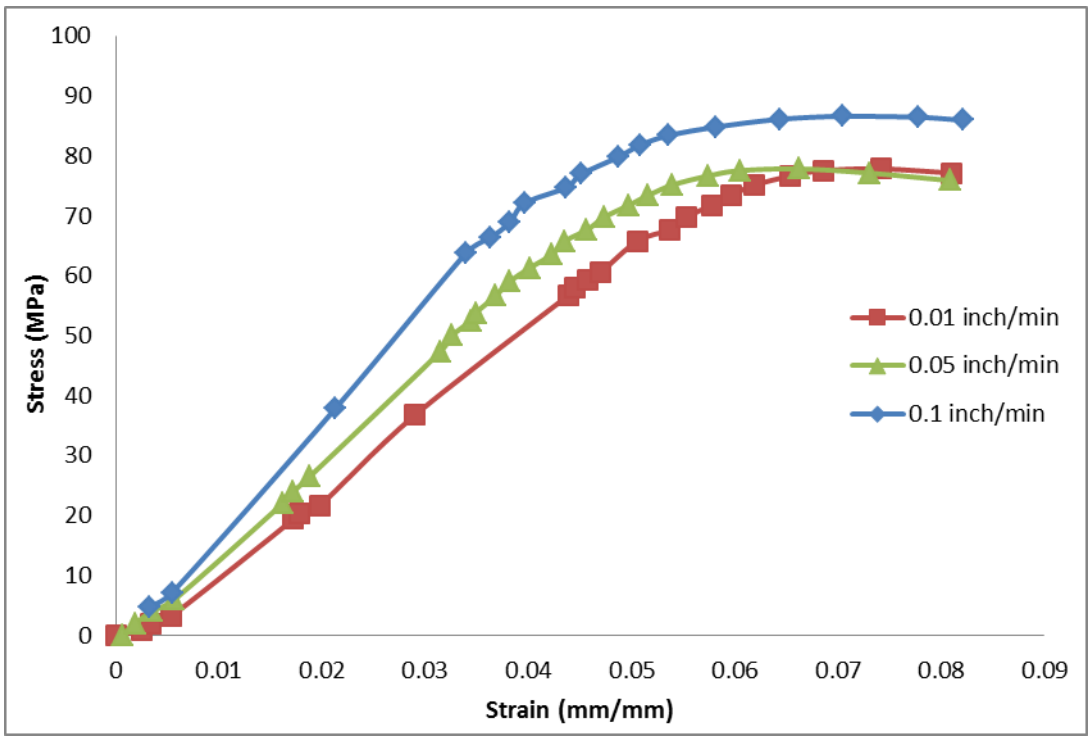

Fig.21. Stress-strain profile of compression test of cylinder specimens

Since, the data from the tensile data is fluctuating more; we used our compression data for further analysis in this study. It is inherent that, the specimens are defective due to the nature of 3D printing. This mode of fabrication would always have some amount of porosity which can affect the mechanical properties of materials by many orders. As the sample size increases, the probability that specimen will have more defects than smaller one. Cylinder samples that we made are very small compared to the tensile sample and that data obtained is more reliable. And, hence the data from the compression test were used for the further study of structures. A cross-section of the samples after the tension test is shown below to see the mode of fracture.

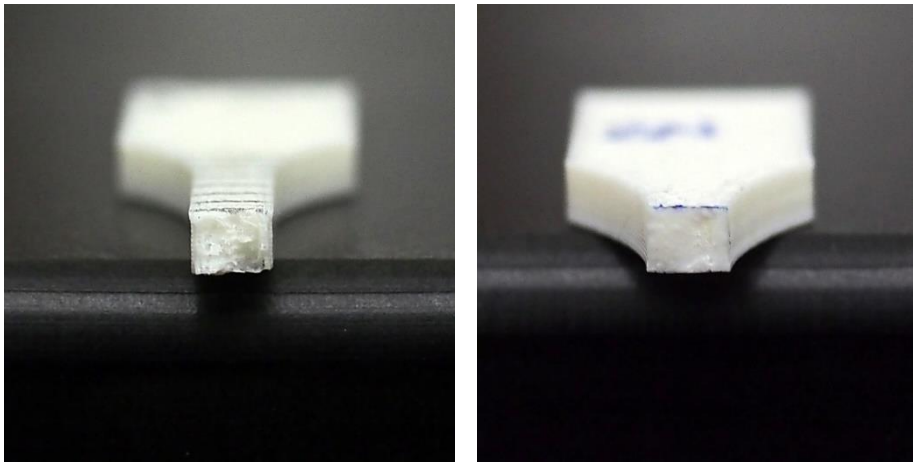

Fig.22. Fractured surfaces of dog-bone specimens after tensile testing

The fractured surface of the specimen showed the brittle nature of the PLA material and the voids suggest that the material has defects especially porosity. And this is no wonder why the samples are behaving differently under tension test. Observed differences between the actual PLA material and printed one is noted.

Material Property	**PLA-original**	**PLA-printed (measured)**
Young's Modulus (GPa)	3-3.5	1.5-1.7
Yield Strength (MPa)	60-65	51.2
Density (g/cc)	1.235	1.10

Table 3: Comparison of mechanical properties of PLA-original and printed PLA

This properties difference is evident to show that the specimens prepared using this fabrication process are defective.

4.2 Analysis of triangular honeycomb structures through experiments and simulation

4.2.1 Experimental

Cellular triangles showed a good response to quasi-static compression tests performed for in-plane in both X and Y directions. The structures showed a stiffness of 569 MPa and 565 MPa in X and Y directions respectively. However, due to the limitation of the experimental tool we had, we could go only 1000 pound force per inch where no deformation pattern can be observed. Figure 23 shows the stress-strain profile of compression in Y-direction at a rate of 0.05 inch/min which just starting to yield at 0.045 ε.

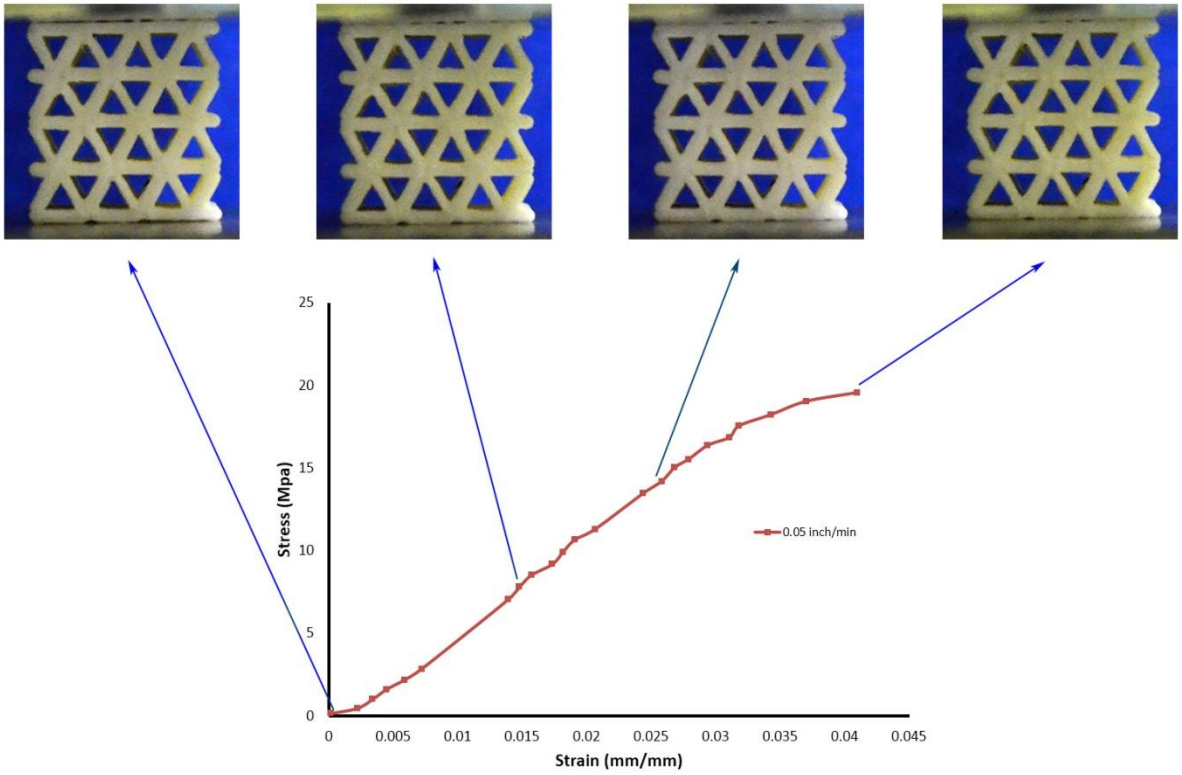

Fig.23. Stress-strain graph of in-plane compression along Y-direction.

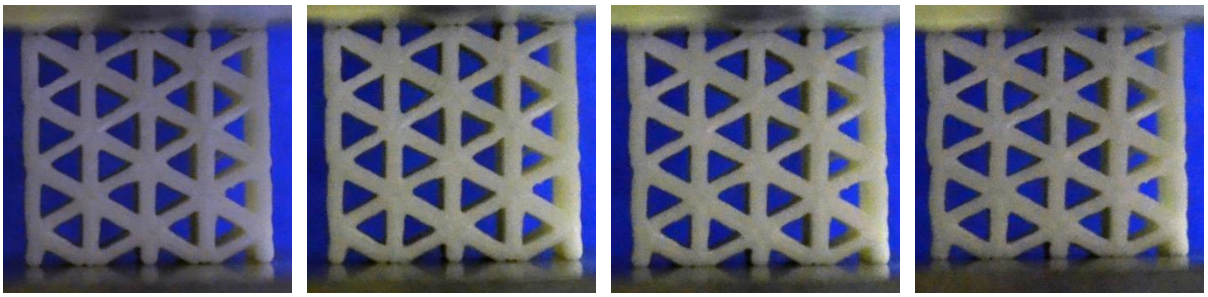

0.01 ε 0.02 ε 0.03 ε 0.04 ε

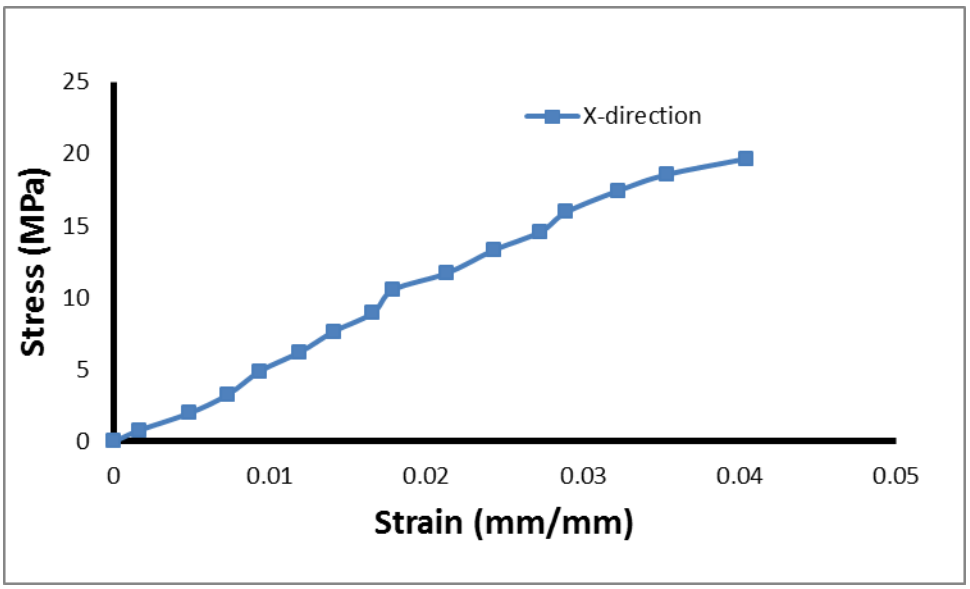

Fig.24. Stress-strain curve in X-direction

The above figure shows the stress-strain profile in X-direction. For the same load, although both directions showed a similar stiffness, yielding starts lower stress in the X-direction than in the Y-direction. The stresses pile-up along the length of straight walls, as we can observe the sides of the specimen started to distort (in 0.03 & 0.04 ε figures) which is the weakest zone in this direction.

4.2.2 Simulation

Unlike the experiments, we went up to 30 % strain in-plane compression during the simulation and observed deformation mode in both X and Y directions. Simulations were done using the material properties obtained from the above cylinder compression test.

X-direction:

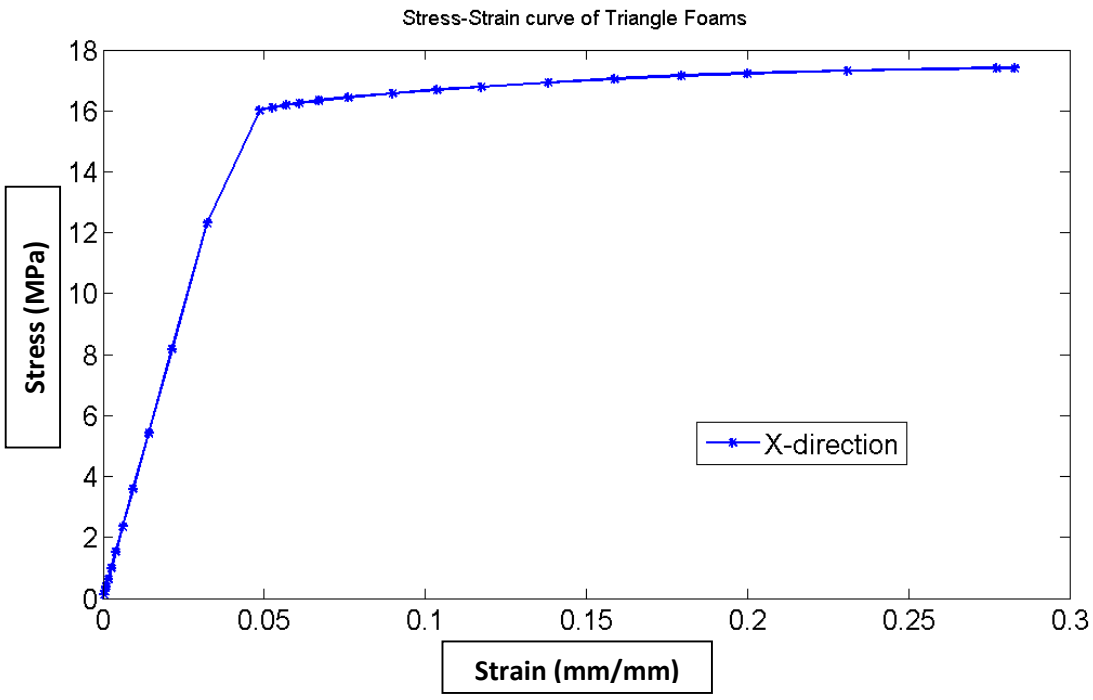

Fig.25. Stress-strain profile of simulated triangle in X-direction

According to the simulation results, the yielding started after 13 MPa in X-direction and th stiffness is 380 MPa which is lower than that of the experimental results. Figure 26 shows the finite element models of cellular triangle structure under in-plane compression at various strain rates. The stress intensity is depicted by the variation of color (Red –highest, Blue-lowest). As the models suggests, the stress initiated along the straight cell walls (showed as in green color at 0.06 ε), as the stress is sufficient enough (shown as red), it started deforming by crewing up stresses to the corners of the triangle edges as shown in figure at 0.3 ε and thus weakens the structure.

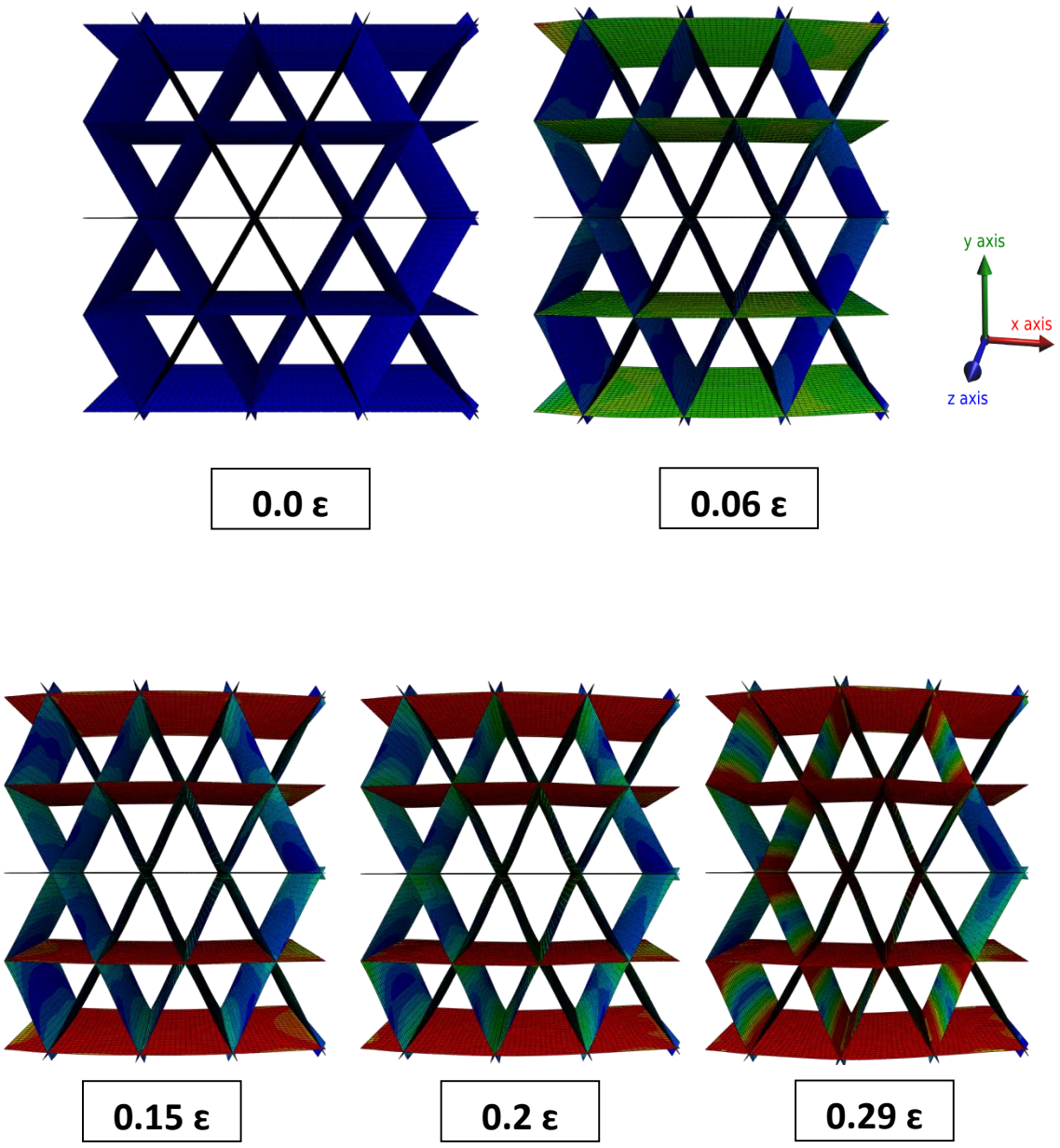

Fig.26. Finite element models of the simulated cellular triangle structure compressed in-plane in X-direction at increasing strains.

Y-direction:

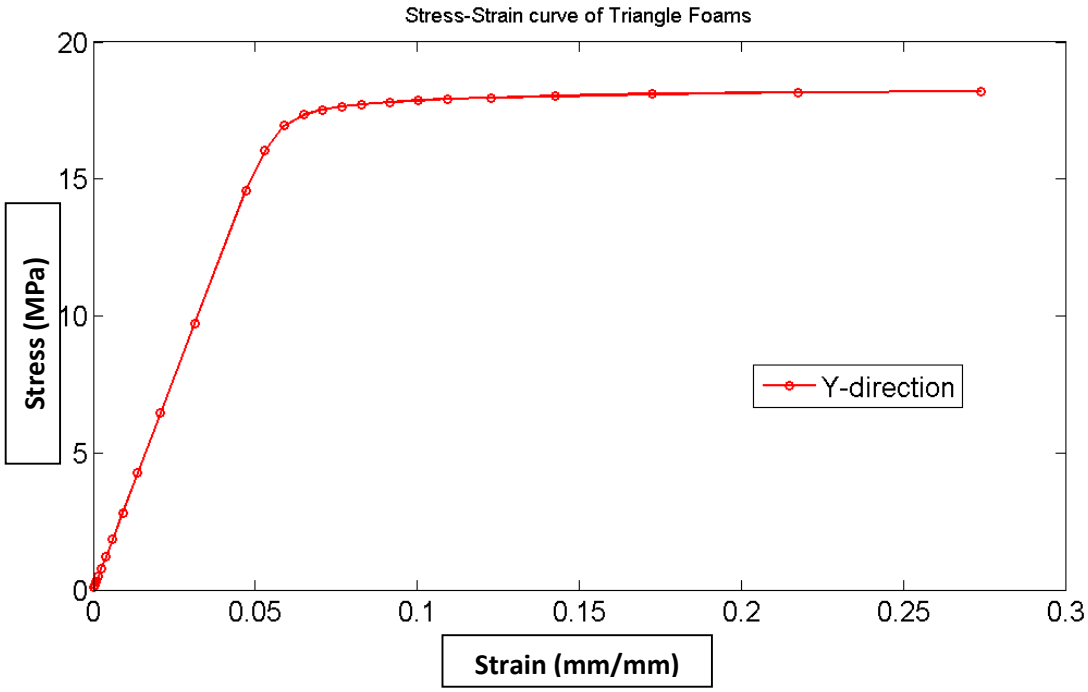

Fig.27. Stress-strain profile of simulated cellular triangular honeycomb in Y-direction

The yield strength and stiffness in Y-direction are 15.2 and 310 MPa respectively from the simulation results. Stiffness is low in Y-direction, whereas the yield strength is more than in X-direction. Fig 27 shows the finite element models of cellular triangle structure under in-plane compression at increasing strain rates. In Y-direction, stress concentration begins along the inclined edges of the triangle cells (observe 0.06 ε in Fig. 27). This cell wall bend around their vertices during crushing as the stress piles up, propagates into next row or cell and thus forms shear bands which can observed at 0.3 ε in the Fig. 27

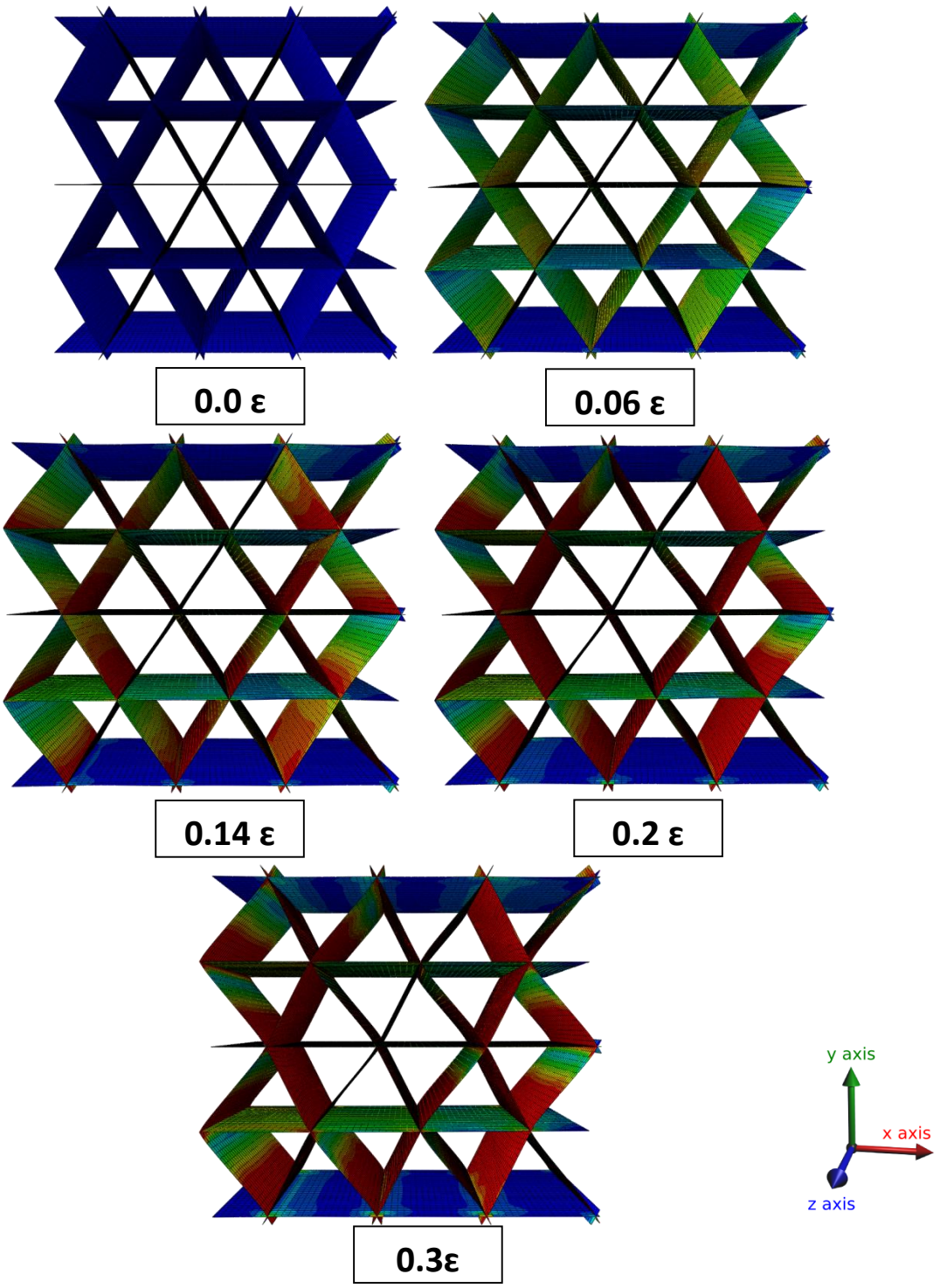

Fig.28. Finite element models of the simulated cellular triangle structure compressed in-plane in Y-direction at increasing strains.

4.2.3 Comparison

Stress-strain profiles of both experiments and simulation are kept together in Fig. 26 and Fig. 27 for comparison. Table 4 below shows the summary of experimental and simulation results.

Cellular Triangle		Experiment	Simulation
X-direction	Yield Strength (MPa)	19	13.5
	Stiffness (MPa)	569	380
Y-direction	Yield Strength (MPa)	21	15.2
	Stiffness (MPa)	565	310

Table 4: Summary of results in experiments and simulations in both X and Y directions

From the table and figures, the specific compressive stress-strain relations together with the sequences of deformations for triangular PLA cellular can be depicted. It is evident that the profiles of the curves in experiments and simulations followed a similar trend. In an actual theory, it is true X-direction has stiffness than in Y-direction which was well proved with the experiment and simulation results too. The mechanical properties obtained from the simulation results are expected to be higher than the experimental results. Since, the material or fabricated model is defect free when we run simulation; the results of simulations are naturally expected to be higher. However, the vice versa has happened (see Table 4 for comparison)

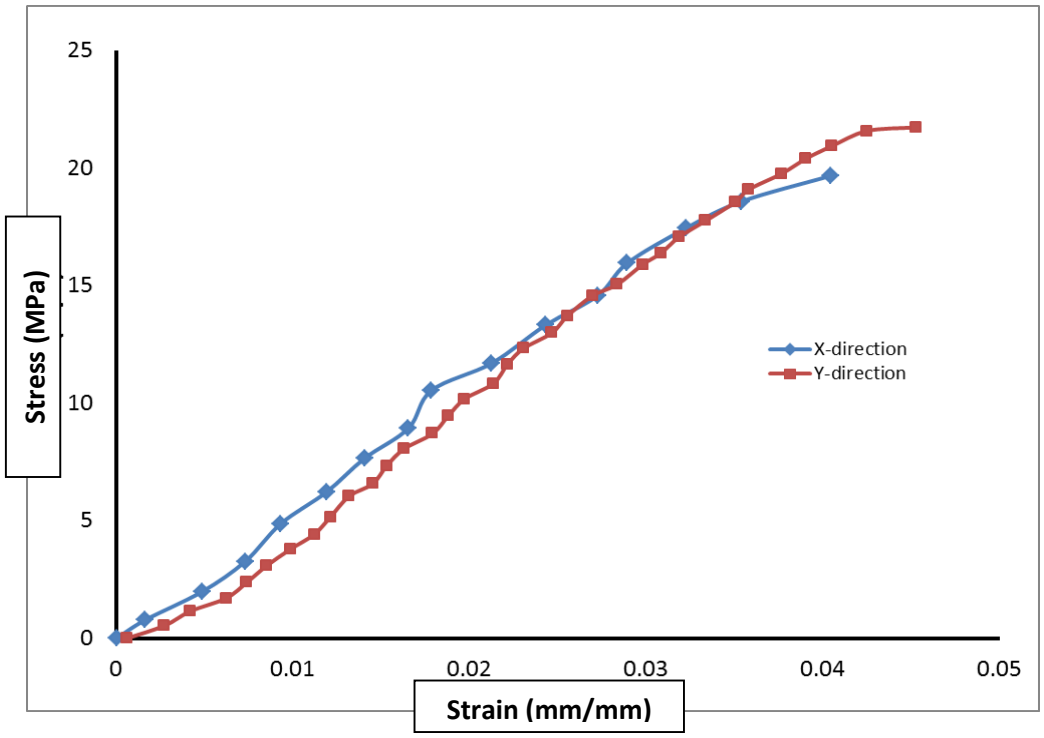

Fig.29. Experimental Stress-Strain profiles of cellular triangle in X and Y directions

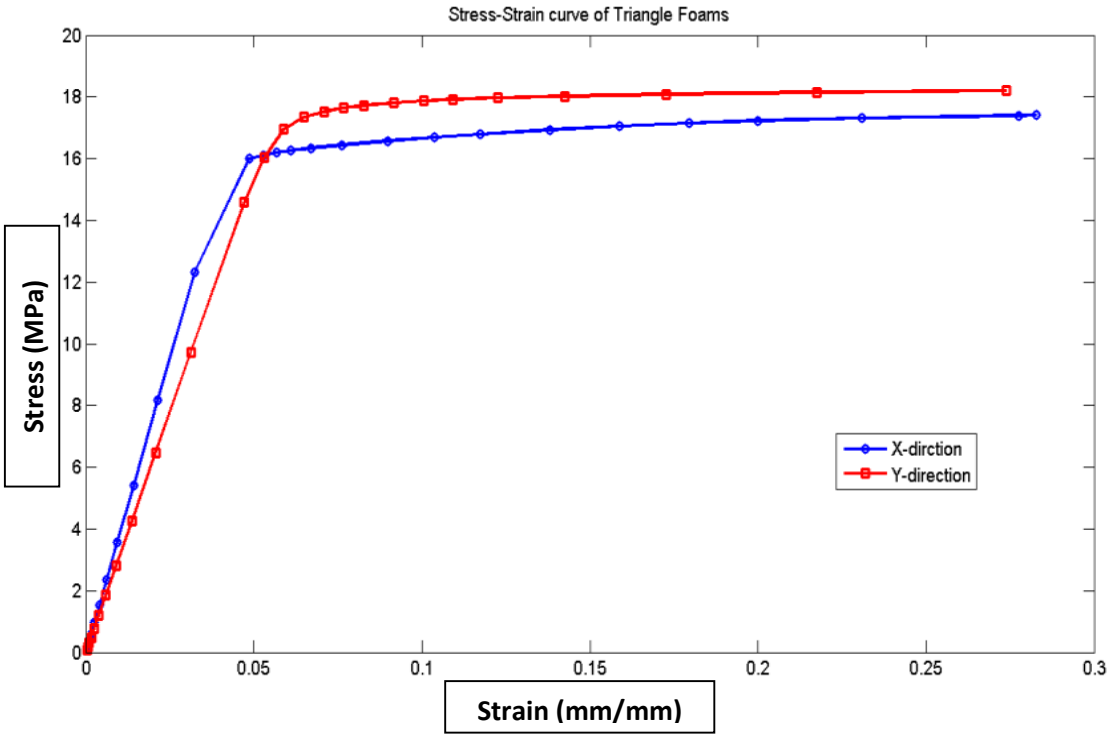

Fig.30. Simulated Stress-Strain profiles of cellular triangle in X and Y directions

This made us look back again in to the fabrication process. As we know that the samples fabricated from the 3D printer are defective with porosity, it is also observed that the thicknesses of cell walls of the sample are thicker than of the CAD file (Fig 28). A dimensional tolerance of 1.5 to 2 % is observed.

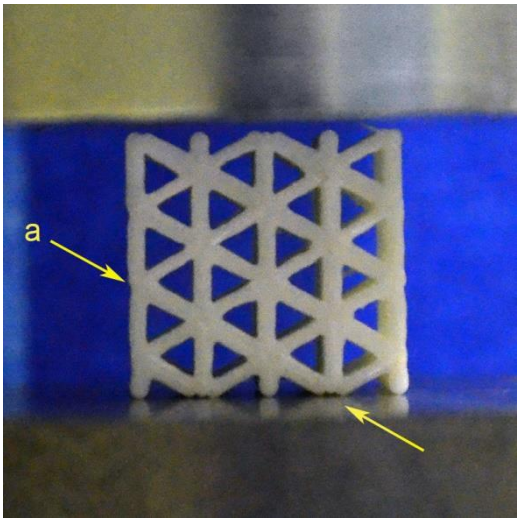

Fig.31. Pointed direction of the plane which looks thicker than other walls

This means that the manufacturing technique has its own limitations in maintaining a uniform thickness of the sample, especially printing small structures. Cell wall dimensions play a very important role in the mechanical properties of the cellular materials and vary in several orders even with minute change in the dimensions of the cell. If the cell wall thickness is given that is measured after printing the structure, the results of the simulation will be higher than the experiments.

Overall, the calculated responses of simulations are in a good agreement with the experimental results. Playing with thickness of the cell walls and printed PLA material mechanical properties during simulation can yield results that will have a very good agreement with the experimental data.

5. Conclusions

In the present work:

1. Poly lactic acid (PLA) was used as a model system to investigate the mechanical behavior of 3-D printed foams with triangular cells.

2. Solid PLA tension and compression specimens and foams made of PLA were fabricated using fused deposition 3-D printing technique.

3. The solid PLA tension specimens were characterized for their densities and found to be about 10% lower in density as compared to their bulk counter parts. The triangular foams had a relative density of about 64%.

4. The relationships between the structure of the foams and its deformation behavior under compression along two in-plane directions were characterized.

5. Simple finite element models were developed to understand the observed deformation behavior of triangular foams.

References:

1. **Iha, Rhiannon K, et al**. Applications of orthogonal “click” chemistries in the synthesis of functional soft materials. Chemical reviews 109.11 (2009): 5620-5686.

2. **Hutmacher, D. W. Schantz, T. Zein, I. Ng, K. W. Teoh, S. H. and Tan, K. C. (2001),** Mechanical properties and cell cultural response of polycaprolactone scaffolds designed and fabricated via fused deposition modeling. J. Biomed. Mater. Res., 55: 203–216.

3. **James Lunt**, Large-scale production, properties and commercial applications of polylactic acid polymers; Polymer Degradation and Stability Volume 59, Issues 1–3, 3 January 1998, Pages 145–152.

4. **Mohamed Naceur Belgacem, Alessandro Gandini,** Monomers, Polymers and Composites from Renewable Resources Book, Elsevier, Oct 2011, Pages 430-434.

5. **Russell A, Benjamin M. Wu, Scott W. Borland, Linda G. Cima, Emanuel M. Sachs, Michael J. Cima,** Mechanical properties of dense polylactic acid structures fabricated by three dimensional printing Journal of Biomaterials Science, Polymer Edition Vol. 8, Iss. 1, 1997.

6. **Rezwan, Q.Z. Chen, J.J. Blaker, Aldo Roberto Boccaccini**, Biodegradable and bioactive porous polymer/inorganic composite scaffolds for bone tissue engineering, Biomaterials Volume 27, Issue 18, June 2006, Pages 3413–3433.

7. **A. Butscher, M. Bohner, S. Hofmann, L. Gauckler, R. Muller,** Structural and material approaches to bone tissue engineering in powder-based three-dimensional printing, Acta BiomaterialiaVolume 7, Issue 3, March 2011, Pages 907–920.

8. **M. Nishida, M. Yamaguchi,** Evaluation of dynamic compressive properties of PLA polymer blends using split Hopkinson pressure bar, DYMAT 2009 (2009) 909–915.

9. **Giordano, Russell A., et al**. "Mechanical properties of dense polylactic acid structures fabricated by three dimensional printing." Journal of Biomaterials Science, Polymer Edition 8.1 (1997): 63-75.

10. **Gibson, L. J.,** et al. "The mechanics of two-dimensional cellular materials" Proceedings of the Royal Society of London. A. Mathematical and Physical Sciences 382.1782 (1982): 25-42.

11. **Henry Tan and S. Qu,** IMPact of Cellular Materials

12. **Gibson, Lorna J., and Michael F. Ashby.** Cellular solids: structure and properties. Cambridge University press, 1999.

13. **Reid SR, Peng C**. Dynamic uniaxial crushing of wood. Int J IMPact Eng 1997; 19: 531–70.

14. **Tan PJ, Reid SR**, Harrigan JJ, Zou Z, Li S. Dynamic compressive strength properties of Aluminium foams. Part I – experimental data and observations. J Mech Phys Solids 2005; 53:2174–205.

15. **Honig A, Stronge WJ**. In-plane dynamic crushing of honeycomb. Part I, crush band initiation and wave trapping. Int J Mech Sci 2002; 44:1665–96.

16. **Ying Liu, Xin-Chun Zhang**, The influence of cell micro-topology on the in-plane dynamic crushing of honeycombs Volume 36, Issue 1, January 2009, Pages 98–109.

17. **Grediac, M.** A finite element study of the transverse shear in honeycomb cores. International Journal of Solids and Structures 30.13 (1993): 1777-1788.

18. **Kanyatip Tantikom and Tatsuhiko Aizawa,** Compressive Deformation Simulation of Regularly Cell-Structured Materials with Various Column Connectivity; Materials Transactions, Vol. 46, No. 6 (2005) pp. 1154 to 1160.

19. **Zhao, Han, and Gérard Gary** On the use of SHPB techniques to determine the dynamic behavior of materials in the range of small strains, International Journal of Solids and structures 33.23 (1996): 3363-3375.

20. **Pervin, Farhana, and Weinong W. Chen.** "Dynamic mechanical response of bovine gray matter and white matter brain tissues under compression" Journal of biomechanics 42.6 (2009): 731-735.

21. **Van Sligtenhorst, Caleb, Duane S. Cronin, and G. Wayne Brodland** "High strain rate compressive properties of bovine muscle tissue determined using a split Hopkinson bar apparatus." Journal of biomechanics 39.10 (2006): 1852-1858.

22. **W. Chen, F. Lu, and B. Zhou** A quartz-crystal-embedded split hopkinson pressure bar for soft materials. *Exp. Mech.*, 40:16, 2000.

23. **Song, Bo, and Weinong Chen**. "Split Hopkinson pressure bar techniques for characterizing soft materials." Latin American Journal of Solids and Structures 2.2 (2005): 113-152.

24. **H. Kolsky**. An investigation of the mechanical properties of materials at very high rates of loading *Proc. Phys. Soc. London*, B62:67, 1949.

25. **Gray III, George T. Rusty.** "High-Strain-Rate Testing of Materials" Characterization of Materials (1997).

26. **L. Wang, K. Labibes, Z. Azari, and G. Pluvinage**. Generalization of split hopkinson bar technique to use viscoelastic bars. *Int. J. IMPact Eng.*, 15:669-686, 1994.

27. **Ballantine Jr, David S., and Hank Wohltjen.** "Use of SAW devices to monitor viscoelastic properties of materials." Ultrasonics Symposium, 1988. Proceedings. IEEE 1988. IEEE, 1988.

28. **W. Chen, F. Lu, D. J. Frew, and M. J. Forrestal** Dynamic compression testing of soft materials. asme trans. *J. Appl. Mech.*, 69:214-223, 2002.

29. **O. A. Shergold, N. A. Fleck, and D. Radford**. The uniaxial stress versus strain response of pig skin and silicone rubber at low and high strain rates. Int. J. IMPact Eng., 2005.

30. **B. Song, W. Chen, and T. Weerasooriya**. Quasi-static and dynamic compressive behaviors of s-2 glass/sc15 composite. J. Compos. Mater, 37:1723-1743, 2003.

31. **Brancazio, David, et al.** "Three-dimensional printing techniques." U.S. Patent No. 5,387,380. 7 Feb. 1995.

32. **Lam, Christopher Xu Fu, et al.** "Scaffold development using 3D printing with a starch-based polymer." Materials Science and Engineering: C 20.1 (2002): 49-56.